Version of Record: https://www.sciencedirect.com/science/article/pii/S0306454920303066
Manuscript_f0c77fbd2d6d7d091656c8579beb287b

Jared Magnusson, Matthew Memmott, Troy Munro
Nuclear MSR Research

Review of Thermophysical Property Methods Applied to Fueled and Un-Fueled Molten Salts

Abstract

Recent investigation into designs of molten salt reactors (MSR) requires accurate data of candidate salts. Review of the literature shows lacking thermophysical (TP) property data for coolants and fuel-bearing salts of Advanced High Temperature Reactors (AHTR). Measurement uncertainties of current data are even more deficient, and this affects ongoing research where MSR modeling and testing are being performed. Melting temperature, viscosity, density, specific heat capacity, and thermal and electrical conductivity measurements are often not arranged together or discussed in great detail, especially for fuel-bearing salts. Raw data from key findings spanning over 70 years for LiF, LiF-BeF_2, LiF-NaF-KF, KCl-$MgCl_2$, KF-ZrF_4, and NaF-KF-MgF_2 have been organized and presented here. Brief description of methods used to obtain these results, in addition to the TP data of some of these salts as fuel carriers, has also been discussed. Thermal conductivity data are particularly weak due to older, high-error measurement techniques. More recent measurement systems to evaluate salt thermal conductivity show promise for obtaining consistent absolute values. This paper concludes that measurement systems such as transient hot-wire method, forced Rayleigh scattering, and laser flash analysis provide the most promise to fill these data gaps and reduce current uncertainty in thermal conductivity measurements of both fueled and un-fueled molten salts.

Introduction

In the last two decades, there has been a renewal of interest in molten salt reactors (MSRs) using chloride and fluoride eutectics. Several US institutions, including Oak Ridge National Laboratory (ORNL) [1], Idaho National Laboratory (INL) [2], and Sandia National Laboratory (SNL) [3] have explored the validity of molten salts as coolants for molten salt reactor concepts. Molten fluoride salts and their heat transfer characteristics are of significant interest in the development of a class of proposed Gen IV reactors because of the salts' high specific heat, low vapor pressure, high boiling point, relatively low melting point, and neutron transparency. The advantages of MSRs over the current fleet of reactors are the inherent safety mechanisms designed into the reactor, the negative coefficient of reactivity, the higher operating temperatures which yield higher thermodynamic efficiencies, lower pressure operation, and the ability to be used with either pebble or aqueous fuel [82-83]. In these reactors, LiF-BeF_2 (FLiBe) is a molten salt of interest [4] for use as the primary coolant fluid because of the favorable thermal properties, neutron transparency, and previous use in the MSRE. LiF-NaF-KF (FLiNaK) is also of great interest because of its similarities to FLiBe while not being toxic, but it has not been proven in full reactor conditions.

Multiple review articles have been published recently to cover thermophysical properties of molten salts, mainly focused on density, heat capacity, viscosity, thermal conductivity, and Prandtl number. Sohal's review [81] presented engineering correlations without the raw data. Romatoski's review [5] presented both correlations and experimental data with reported uncertainties where available but did not discuss the role of systematic uncertainty in the methods, nor were fuel containing salts considered. Assael's review focused on a particular property (thermal conductivity) to establish useful correlations on molten nitrate, bromide, iodide, and chloride, salts, but no results are presented on

© 2020 published by Elsevier. This manuscript is made available under the Elsevier user license
https://www.elsevier.com/open-access/userlicense/1.0/

fluoride salts [6]. Clarno et al offered a comprehensive review of different properties (sans electrical conductivity) for multiple coolants, but again no fuel bearing salts were reported upon [7].

Though some thermophysical properties of fluoride salts have recently been measured [79], there is still much that is left wanting, especially for properties at temperatures near proposed MSR operation (~700 °C). Additionally, most legacy data (originally obtained while the MSRE at Oak Ridge was in operation) does not include salts that contain nuclear fuel (particularly UF_4). For example, for thorium containing salts, the measurement of thermal conductivity near the MSR operating temperature by ORNL is data at a single temperature of the fertile material LiF-ThF_4 [8].

This review will focus on the summary of experimental data from over 70 years of thermophysical properties of the following salts: LiF, LiF-BeF_2, LiF-NaF-KF, KCl-$MgCl_2$, KF-ZrF_4, and NaF-KF-MgF_2. The properties considered will be thermal conductivity, heat capacity, density, electrical conductivity, viscosity, and melting point for both coolant and fueled salts in light of the potential errors based on the methods used to obtain the data. Properties such as surface tension and vapor pressure are not included. Unique to this review is the inclusion of fuel salt properties where available, as well as a discussion of the experimental methods used to obtain the data and reported experimental uncertainties. Of particular note is the literature on thermal conductivity (k) of the salts because of the observed increase in k with increasing temperature, while typical salts and fluids exhibit a decrease in thermal conductivity with increasing temperature. This discrepancy demonstrates the need for improved accuracy in experimental methods to determine if the increasing k is due to un-accounted for radiation and convective heat transfer or if there is some mechanism in the salt that gives rise to this behavior.

1. Determination of Candidate Salts

Because this review article is focused on compiling data on molten salts for use in Molten Salt Reactors (MSRs), nitrate salts were not considered. It is worthwhile to briefly describe the necessary considerations for molten salts in both a primary heat producing loop and a secondary cooling loop, and then to identify promising candidate salts and their most crucial thermophysical properties.

With respect to nuclear reactor concepts, many coolants have been proposed, ranging from light water and heavy water in current generation reactors, to gas, sodium, and salt in advanced reactor concepts. Although there are benefits and disadvantages to each type of coolant, there are significant advantages to utilizing a molten salt as a working coolant or fuel medium with respect to heat transport and safety. These include a high working temperature for a high power conversion efficiency, a high volumetric heat capacity for a compact design with minimal temperature transients, a high vapor pressure facilitating low operating temperatures, and a low reactivity with air and water to prevent energetic pipe-break accidents [9]. Disadvantages of using molten salts include the highly corrosive nature of these salts [10], as well as potentially high complexity and cost of producing and purifying the molten salts [11]. Despite these challenges, there is high interest in commercializing nuclear reactors cooled by molten salt, and these efforts focus on a variety of salts and technologies at a wide range of technology readiness levels [12].

Although the molten salt reactor experiment (MSRE) and subsequent breeder concepts which pioneered molten salt reactor technologies utilized primarily fluoride salts, a growing interest has arisen in using chloride salts as fuel or coolant salts. This interest is focused primarily in the ability of chloride salts to cool the reactor without moderation, facilitating a fast reactor salt concept [13]. In addition to this advantage, chloride salts tend to have the same ideal thermohydraulic features as a chloride salt, though they typically have lower melting points and cheaper, simpler fabrication and handling procedures due to the lack of beryllium and lithium. Despite these benefits, however, a setback to the chloride salts is that the chemistry of these salts is more complex and less well understood [14]. Based on these considerations, it is possible to design a viable molten salt reactor with either fluoride or chloride salts, and thus both salts must be considered when determining ideal candidate salts.

Two major MSR designs are under consideration in this paper. The first is a fluoride salt-cooled high temperature reactor (FHR) where solid fuel transfers heat through a primary salt coolant to a secondary salt coolant for power generation [15] (Figure 1). The second is typically just called an MSR with fuel bearing salt as the primary loop and a coolant salt in the secondary loop.

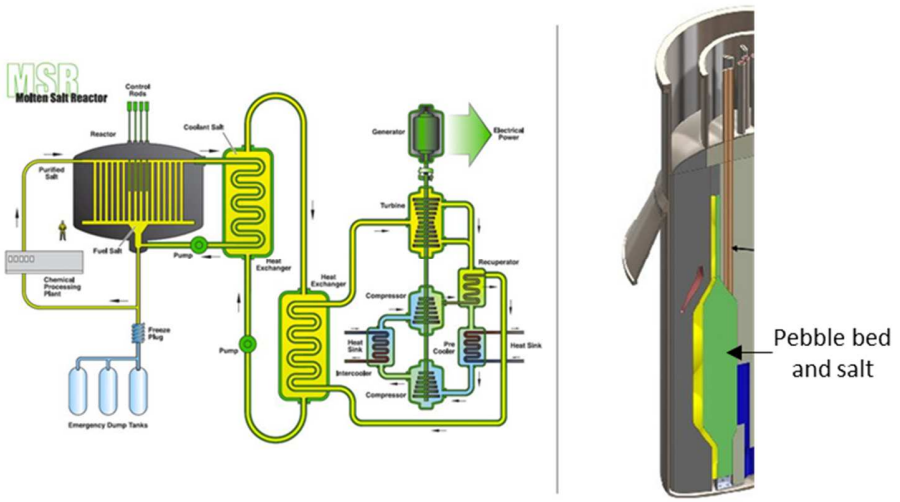

Figure 1 Schematic of MSR versus FHR. The MSR (left) uses fuel-bearing salt in the primary loop which then passes heat to a secondary coolant. In an FHR (right), solid fuel pellets transfer heat to a primary coolant, much like in a pressurized water reactor (PWR). Images courtesy of [16] (left) and adapted from [17] (right).

It should be noted that despite many different designs that have been proposed in both the MSR and FHR configurations, no molten salt reactors have yet been licensed for commercial operation worldwide [18]. In part, this is due to the lack of a licensing framework for advanced reactors, and in part due to the large amount of uncertainties that still exist regarding the use of molten salts as coolants and fuel carriers. Although licensing considerations are beyond the scope of this paper, it should be noted that salt selection and subsequent behaviors will play a significant role in safety assessment and licensing efforts. Thus, the authors seek to call attention to the fact that significant efforts are being undertaken to both modernize the licensing process for advanced reactors in general [19], as well as specific efforts to modernize and understand licensing requirements for MSR and FHR designs [20]–[22].

Coolant Salts

The 2017 Molten Salt Workshop [23] defined general coolant salt requirements and how they differ from necessary fueled-salt (primary loop) properties discussed later. For use as primary, coolant salts, negative void and temperature coefficients are desirable, which can be accomplished when salts possess a small neutron cross section, as in the case of FLiBe's -$0.11 coolant void ratio with an Er_2O_3 poison [24]. Radioactive byproducts must also be accounted for, such as the production of tritium with FLiBe when using ^{6}Li. Compositional changes throughout the heating cycle must be minimized as vapor pressures are highly sensitive to such fluctuation, though most vapor pressures are extremely low to begin with [25]. Hydrodynamic and heat transfer properties become a higher priority when dealing with coolants in the secondary loop because radiation and fission product exposure is less of a factor. Thus, further attention can be paid to minimizing pumping losses and heat transfer. Even electrical conductivity has an effect upon transport properties and suitable test equipment. For example, Clarno et al [7] stated that the density of the salt had little effect on suitability, but a greater density may make heat removal by natural convection better. However, too high of density or viscosity burdens pumping capabilities. Considerations such as these cannot be made without accurate experimental data.

Coolant salt compositions were chosen in the eutectic phase because it ensures uniformity in salt properties when in operation and often represents the composition with the minimum melting point. When multiple eutectics were possible, especially for the ternary salts, the eutectic with the lowest melting point was considered in this paper.

Fuel-Salts

When molten salt contains fissionable fuel (fuel-salt), additional criteria must be considered when investigating its properties [23]. The fuel must dissolve fissile, fertile, and fission products, while maintaining an acceptable variation of its properties for steady behavior [23]. Stability in the presence of high temperatures and radiation fields, while maintaining low vapor pressure, is critical [23]. Heat transfer and hydrodynamic properties such as heat capacity and viscosity need to be considered across the reactor's operating temperatures in order to minimize complications to pumping mechanisms and avoid premature maintenance on turbomachinery. Additional economic considerations for material refinement must also be considered but are outside the scope of this paper.

Grimes et al [26] goes into detail in selecting melting points for salt-fuels. A maximum operating reactor temperature of 936 K would be sufficient to account for a margin of error when dealing with the critical temperature for the salt-alloy interface. Due to potentially high changes in temperature at the heat exchanger (up to 56 K), a maximum melting point of 823 K (550 °C) would hinder precipitate formation with margin in the salt during operation. Sohal et al [27] recommended a melting point less than 798 K (525 °C).

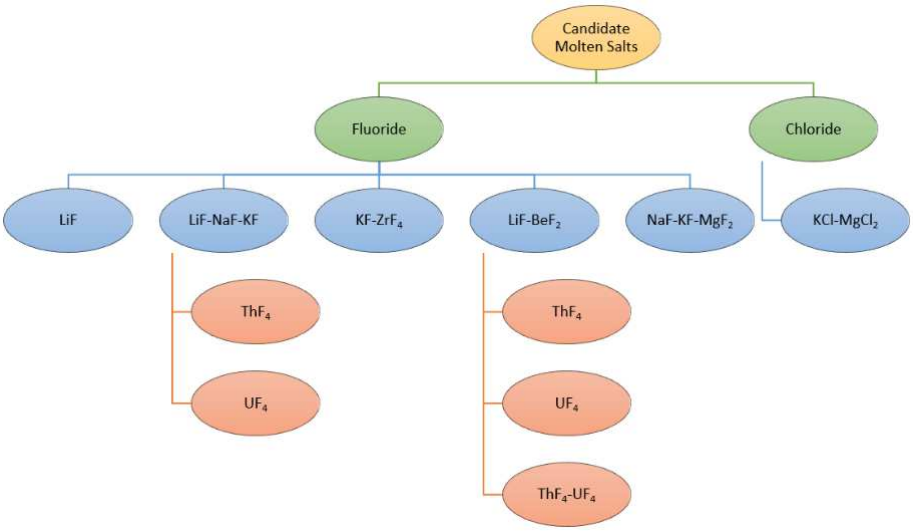

Figure 2 Hierarchy of molten salts examined in this paper. Only FLiBe and FLiNaK were examined as potential fuel carriers.

Candidate Salts

Ten molten salts were examined in this paper, of which only one was a chloride salt (Figure 2). General property ranges for liquidus salts are given in Table 1. Note that in Table 1, all values except those for melting point are the result of experiment. Specific salts considered are as follows:

LiF: Lithium fluoride is the base component of many salts in this review. While its individual properties are not as competitive as those of some of the following binary and ternary salts, it has been considered as a fuel bearing salt due to its ability to carry a higher concentration of uranium than LiF-BeF_2[15]. It has been mixed with both uranium and thorium tetrafluoride as well as a combination of the two. While LiF fueled salts have been discussed for MSR use, these fuels will not be discussed here, though discussion of measurement methods and results obtained in sections 2-4 can be directly applied to them.

LiF-BeF_2 (FLiBe): While pure LiF is able to dissolve a greater concentration of uranium than FLiBe, LiF has a much higher melting point and poorer neutron moderating properties [15], [28]. FLiBe possesses a low corrosion rate when uncontaminated and boasts an extremely low neutron cross-section, toxicity notwithstanding[15]. However, its high cost due to the refinement of ^7Li makes it a cost effective coolant only when used in the primary loop due to its favorable thermophysical properties[7]. To avoid high vapor pressures, Clarno et al [7] recommends FLiBe with a molar BeF_2 concentration less than 35 – 45%. Because of its ability to dissolve ThF_4 and UF_4 in any composition, FLiBe may be best suited as a fuel-bearing salt. This work presents properties of FLiBe as a coolant salt, in addition to compositions containing either ThF_4, UF_4, or both (Figure 2).

LiF-NaF-KF (FLiNaK): Like FLiBe, FLiNaK has been the subject of extensive research as to its properties after FLiBe usage in Oak Ridge's Molten Salt Reactor Experiment (MSRE) [29]. While possessing similar thermophysical properties of the former, FLiNaK remains a cheaper solution because it does not necessitate special handling of toxic beryllium [15]. However, Bahri et al [29] noted that while PuF_3 and UF_4 were highly soluble in FLiNaK, FLiNaK possesses a parasitically high neutron capture cross section from its potassium component. Though FLiNaK has been mostly studied in solution with UF_4, this paper briefly considers its properties when containing ThF_4.

KCl-$MgCl_2$: According to Rabald [30], chloride salts have higher vapor pressure and lower volumetric heat capacity than fluorides; however, they also possess lower melting points and possibly less corrosive properties. In addition, chloride salts possess lower viscosities but also lower thermal conductivities [31]. Magnesium chloride salts also carry an enormous cost advantage over their fluoride counterparts by more than a factor of ten [32]. Chloride salts' greatest hindrances remain chlorine activation under neutron absorption (^{36}Cl is a large beta particle emitter) [23] and even less research than that of fluoride salts.

KF-ZrF_4 (FluZirK): Similar to chloride salts, FluZirK offers low toxicity when compared with FLiBe and lower cost due to lack of enriched lithium [32]–[34]. However, the potassium in the KF component, with its nearly 60% molar concentration, has poor neutron transparency [7]. The ZrF_4 concentration governs the vapor pressure of the salt, with 20-45% ZrF_4 concentration necessary to maintain < 1 mm Hg of pressure at 900 °C [7], [25].

NaF - KF - MgF_2: This ternary has been largely unstudied but represents a new direction for MSR design. Due to the almost prohibitive nature of FLiBe's toxicity, cost and the inferior neutronics of its alternatives, Dr. Matthew Memmott's research group at Brigham Young University proposed a new salt possessing model neutronic and thermophysical properties. However, with a melting temperature nearly three times that of FLiBe, Dr. Memmott's team are exploring the idea of freezing the same salt around the walls of reactor piping (a salt wall or barrier) in order to prevent corrosion and melting of typical alloys at NaF-KF-MgF_2's eutectic melting point. Additionally, cooling of the frozen salt wall is unnecessary by using a composition slightly higher than the eutectic in order to increase its melting point. ***Table 1 Experimental molten salt property data.***

	Melting Temperature*	Density**	Dynamic Viscosity	Thermal Conductivity	Specific Heat Capacity, Isobaric	Electrical Conductivity
Symbol	T_m	ρ	μ	k	c_p	σ_e
Units	°C	g/cm^3	mPa-s	W/m-K	cal/g-K	Ω^{-1} - cm^{-1}
LiF	848	1.63 - 1.82	1.38 - 2.21	1.20 - 2.22	0.58 - 0.60	8.16 - 10.41
LiF-BeF_2	458 - 459.1	1.82 - 2.03	1.86 - 13.91	1 - 1.19	0.56 - 0.58	1.34 - 2.51
LiF-NaF-KF	454 - 463.6	1.84 - 2.13	1.30 - 14.44	0.22 - 5.38	0.41 - 0.48	1.07 - 1.79
KF-ZrF_4	390 - 430	2.45 - 2.66	2.34 - 6.95	-	-	-
NaF-KF-MgF_2	685 - 975	-	-	-	-	-
KCl-$MgCl_2$	423 - 440	1.46 - 1.69	2.44 - 6.01	0.54 - 0.63	0.24	0.59 - 0.74
LiF-BeF_2-ThF_4	356 - 485.8	2.64 - 3.66	7.06 - 16.53	-	0.32	1.38 - 2.61
LiF-BeF_2-UF_4	350 - 464	3.74 - 3.93	4.08 - 33.33	-	-	-
LiF-BeF_2-ThF_4-UF_4	480 - 500	2.58 - 3.41†	4.8 - 19.38	1.21 - 1.36	0.33 - 0.39†	1.63 - 5.72†
LiF-NaF-KF-ThF_4	450	1.8 - 2.2†	1.95 - 9.20†	-	0.45†	-

$LiF\text{-}NaF\text{-}KF\text{-}UF_4$	452 - 560	1.8 - 2.5†	1.7 - 9.0	4.0†	0.40 - 0.44	-

*All property values presented here, excluding some melting temperature values and ranges marked with †, are the result of experimentation.

** All measured property values fall in the range of T_m-1000 °C with the exception of LiF (T_m-1300°C).

2. Investigation of Coolant Salt Properties (sans fuel)

This section details the existing thermophysical properties from literature for the candidate salts in Section 1 containing no fissile fuel. Properties include: melting point and at specific molar compositions, density (ρ), viscosity (μ, ν), specific heat at constant pressure (c_p), thermal conductivity (k), and electrical conductivity (σ_e). Data was extracted either directly from experimental tables, equations, figures or listed averages. When research findings were presented in a diagram, GetData Graph Digitizer and WebPlot Digitizer were used for extraction purposes.

Melting Point & Compositions

ORNL's previous MSRE [15] operated at a peak output of 705 °C (978.15 K). Clarno et al [7] stated minimum Brayton cycle temperature constraints, material limits, and opportunity for dry cooling require an operating temperature of at least 700 °C. Thus, all coolants must have melting points far below this value to maintain stable property values at all times. For that purpose, this work will present the standard MSR operating temperature as a range from 923-1023 K (650-750 °C).

Melting points and molar compositions for coolants of interest are listed in Table 2. As observed by Williams [32], extensive research has brought confidence to the phase diagrams of the listed melts, especially the binary salts. However, uncertainty was often unspecified for these values and variation in melting point in the presence of fission products for primary coolants must be sought out.

LiF: Due to it being a unary salt and a key component of several other candidate salts, the melting point of LiF has been well documented. Douglas and Dever employed an extrapolation technique with respect to furnace temperature in order to obtain results with a calculated 0.10% error [35]. Thoma et al reported 1121 K (848 °C) for their melting point using differential thermal analysis (DTA), a temperature later documented by Janz et al with 0.90% error [36], [37]. Review articles such as Sohal et al and Williams often cited a melting point of 845 °C, though their original sources were unspecified [27], [32]. The 2005 CRC handbook reported a melting point of 848.2 °C [38].

FLiBe: Thoma et al [36] summarized almost all previous work dealing with FLiBe's eutectic composition. Thoma et al reported that diversity in FLiBe's phase equilibrium diagrams prior to that publication resulted from error due to hydrolysis, impurities, or metastable nucleation. They formed a new binary diagram from multiple experimental methods and previous works, identifying a peritectic melting point at 458 °C and 34% BeF_2. In 1972, Romberger et al [39] resolved difficulties with impurities using EMF measurements to obtain a more correct equilibria measurement. Romberger found the eutectic point at 32.8% BeF_2 with a melting point of 459.1 °C (0.2% error).

FLiNaK: Bergman and Dergunov [40] were first to publish a eutectic melting point for this mixture. Rogers et al [41] adjusted this value accounting for supercooling effects using DSC with only 2% error. The value cited by Janz and Tomkins [42] is identical to that of Bergman and Dergunov.

KCl-$MgCl_2$: The online FactSage database [43] presented several melting points for this chloride salt, but no detail as to their measurement technique or error were reported. Robertson [44] presented a summary of studies on KCl-$MgCl_2$ and cited differences from various authors regarding its liquidus phases. Seifert and Fink [45] conducted a noteworthy analysis using DTA and possibly X-ray diffraction in their study of magnesium chloride compounds. They found three eutectics, two of which possess sufficiently low melting points to be of interest. Varying $MgCl_2$ molar composition by less than 5% resulted in a 17 K range in melting temperature.

FluZirK: Two melting points are cited for FluZirK: Thoma and Grimes in 1957 [46] and Alekszeeva & Poszipajko [47] in 1977. Both sources had matching eutectic melting points at 55% ZrF_4 but differed considerably with the 42% ZrF_4 eutectic. No measurement method or uncertainty is documented by either, though Thoma and Grimes regarded their phase diagram as "tentative and subject to revision after further study". A lower eutectic temperature of 663 K by Thoma [48] is referenced by Williams [32], [34] in 2006.

NaF - KF - MgF_2: In 1945, Bergman and Dergunov [49] determined melting points for three compositions of the ternary, though the exact method is unspecified.

Table 2 Coolant salt eutectic melting point data reference.

Author	Year	Molar Composition (%)	Technique employed	Uncertainty quoted (%)	Melting Point (K)
		LiF			
Douglas & Dever	1954	100	Extrapolation from furnace temperature	0.1	1121.3
CRC Handbook	2005	100	-	-	1121.4
Janz et al.	1979	100	-	0.9	1121
Thoma et al.	1968	100	DTA	-	1121
		LiF-BeF_2			
Romberger et al.	1972	67.2 - 32.8 (± 0.04 %)	EMF measurements	0.2	732.3
Thoma et al.	1968	68 - 32 63.5 - 34.5	Thermal gradient quenching, Thermal/ differential analysis	-	731.2
		LiF-NaF-KF			
Bergman & Dergunov	1941	46.5 - 11.5 - 42.0	-	-	727
Rogers et al.	1982	46.5 - 11.5 - 42.0	High temperature DSC	2	735
		KCl - $MgCl_2$			
FactSage	-	69.8 - 30.2 65.3 - 34.7	-	-	696 702
Robertson	1966	70 - 30 68 - 32 69.5 - 30.5	-	-	703 699 713
Seifert & Fink	1974	69 - 31 65.5 - 34.5	DTA, X-ray diffraction	-	700 701
		KF-ZrF_4			
Alekszeeva & Poszipajko	1977	53 - 47	-	-	703
Thoma & Grimes	1957	58 - 42 45 - 55	-	-	703 713
Thoma	1959	58 - 42 45 - 55	-	-	663 713

NaF - KF - MgF_2					
Bergman & Dergunov	1945	33.0 - 13.5 - 53.5 62.5 - 15.0 - 22.5 34.5 - 59.0 - 6.5	-	-	1248 1071 958

Density

As stated previously, mass flow rate of the cycle fluid varies directly with density, which affects pumping requirements. Additionally, correct knowledge of density enables determination of the volumetric expansion of the salt, a key parameter in determining heat transfer by natural convection [31]. Density data are also involved in calculating the mass of fissionable products when undergoing pyroprocessing of spent fuel [31]. Density data are provided in Figure 3-Figure 7 and Table 3.

LiF: Density data for LiF are rather prolific, though most results stemmed from binary or ternary salt data where LiF was an isolated component (Figure 3). Jaeger and Khan's early work to determine temperature coefficients of molecular surface energy also resulted in values of specific gravity for many of their studied salts [50]. They employed a hydrostatic method with a platinum sinker submerged in salt. While they did not list an error estimate, they did note uncertainty due to the vapor pressure of the studied salts. Yaffe and Artsdalen reported density values relevant to their work in electrical conductivity, but no information beyond them using a submerged bob method was presented [51]. Blanke et al [52] presented pure LiF data using the 'loss-in-weight' method employing the Archimedes principle, measuring the change in weight of a platinum cylinder when immersed in the molten sample with 1% error [53]. Mellors and Senderoff employed a tungsten bob with 2% error [54] while Hill et al used a platinum plummet with nickel containers [55]. Both of these sources agree extremely well with Yaffe's and Jaeger's work. Porter and Meaker used a molybdenum plummet and quartz-spring balance with highly consistent results [56], but values were further from previous work and more closely aligned with those of Blanke et al.

FLiBe: Most FLiBe density data were based entirely around two major data sets (Figure 4). The first [52] by Blanke et al presented raw data across several compositions, including two nearly eutectic compositions (66.67-33.33 % and 62.67-37.33 %, though only the former is considered here). They again used the 'loss-in-weight' method mentioned previously [53]. Cantor [57] conducted experiments using a nickel dilatometer. Both studies had errors of less than 1% and were in strong agreement with each other, especially when considering compositional differences. Citations of density by Janz [58] are excluded because his results were largely based on the work of Cantor [59], which presented correlations at non-eutectic compositions, though he did achieve density measurements up to 860 °C.

FLiNaK: The correlation by Janz and Tomkins [42] mirrored data from Mellors and Senderoff [54]. Janz and Tomkins reported 2% error for their trend line, and this error is displayed in Figure 5. Most other data and trends originate from calculated values, though Cohen and Jones' experimental data [60] were another source of subsequent equations developed in the literature. Unfortunately, only averages are reported here because exact values were never originally presented. Both Cohen and Mellors employed some variation of the Archimedean method. More recently, Cibulková et al [61] averaged values from one heating curve and two cooling curves to construct their high temperature correlation which agrees with that of Mellors, although no uncertainty was documented. They utilized a platinum plummet suspended by wire from an electronic balance. In 2013, Cheng et al [62] reported nearly 200 data points of FLiNaK density, but data were reported at much lower temperatures than those estimated for MSR operation. Nevertheless, the trends reported by Cheng lend strong support to the accuracy of earlier tests.

KCl-$MgCl_2$: Prolific data has been reported on KCl-$MgCl_2$ and is referenced by Janz & Tomkins [42] and Janz et al [63]. However, much of the data remains unverifiable due to difficulty in finding original publications, thus few could be recovered (Figure 6). The first, by Grjotheim et al. [64], reported a single density value for the composition of interest (67.33-32.67%) at 800 °C. Grjotheim's hydrostatic method involved a thermos-vacuum balance with an estimated error of 0.2-0.4%. Reding [65], reported a correlation for a different molar composition (35.5 % $MgCl_2$) based upon

measurements using the buoyancy method. While no uncertainty was reported, Reding's values agree well with Grjotheim's at 800 °C. Huber et al [66] cited density values at three temperatures, aligning well with Reding's, though over a lower temperature range. More recently, Yuanyuan et al [67] worked to compare available modeling techniques with experimental data using an unspecified Archimedean technique. No uncertainty was detailed, but Yuanyuan's models conformed with experimental values. However, Yuanyuan's model trend line diverged as experimental temperatures decreased.

FLuZirK: Two separate correlations by Darienko et al [68] in 1988 bracket the eutectic composition of interest (Figure 7). Darienko reportedly used the maximum gas-bubble pressure method to determine both density and surface tension with 1% error, though the exact procedure for determining density from this method is unknown. Serrano-López et al [33] interpolated these values to find a fit for the 42% ZrF_4 composition.

NaF - KF - MgF_2: No available density data was found for this salt.

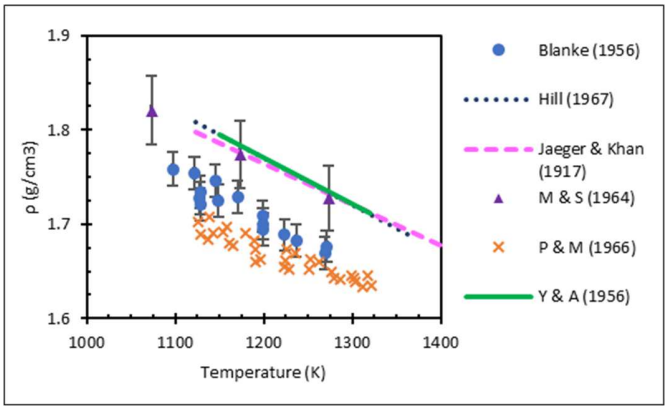

Figure 3 Density as a function of absolute temperature for LiF. Blanke et al. reported 1% error while Mellors and Senderoff (M&S) reported 2%. Hill, Jaeger, Porter and Meaker (P&M), and Yaffe and Artsdalen (Y&A) did not provide an error estimate.

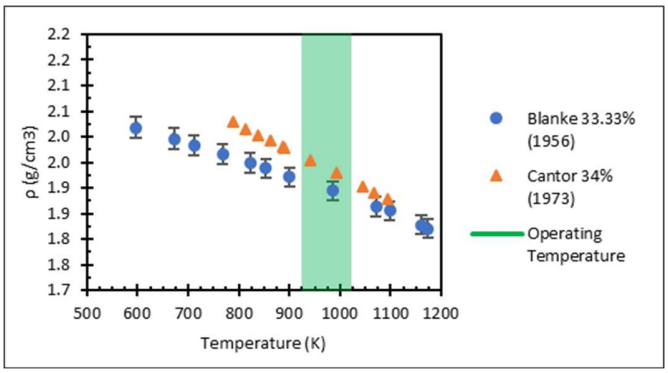

Figure 4 Density as a function of absolute temperature for FLiBe. XX% indicates the percentage of BeF_2 in the composition. Blanke reported 1% error in the measurement while Cantor reported 0.3%, which is omitted for clarity.

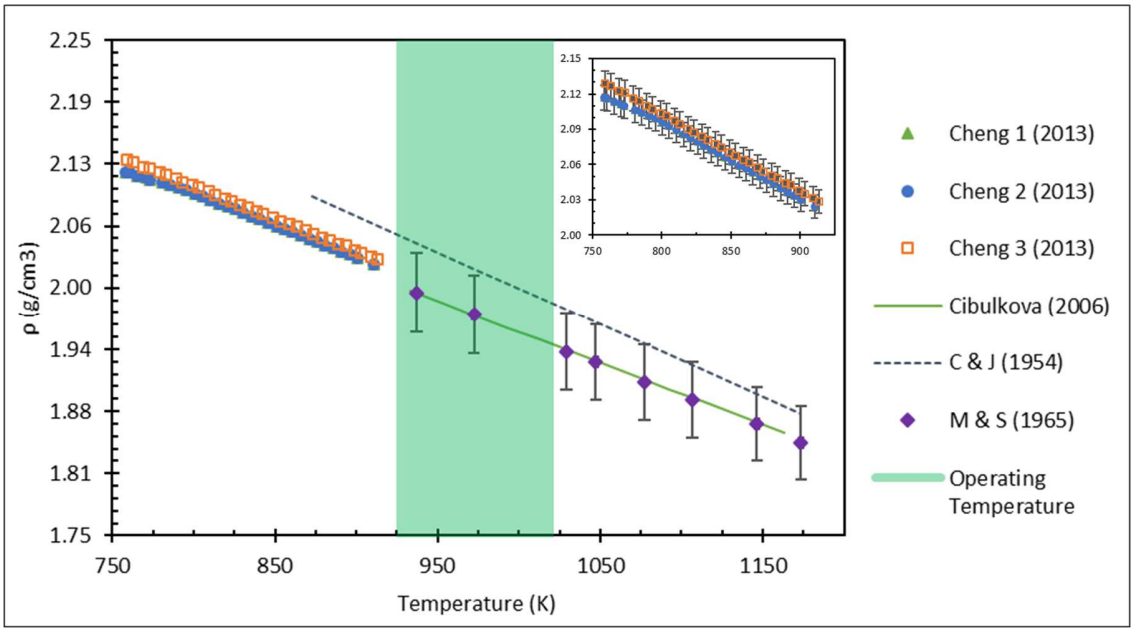

Figure 5 Density as a function of absolute temperature for FLiNaK. Cheng et al ran three tests (Cheng X) which agreed very well with each other and only reported 0.5% error. A separate figure is shown for clarity. Cibulková et al and Cohen and Jones (C & J) reported experimental trend lines, though Cohen and Jones did provide sample values which differed slightly from the correlation (not shown). Mellors and Senderoff (M & S) reported 2% error.

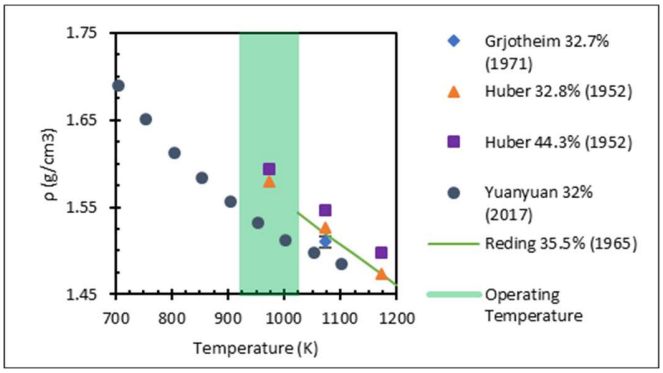

Figure 6 Density as a function of absolute temperature for KCl-$MgCl_2$. XX.X% indicates the percent molar concentration of $MgCl_2$. No work presented error except Grjotheim et al, who reported 0.2-0.4% error (0.4% shown). Reding presented just a trend line, though the values from Huber et al were likely derived from similar correlations.

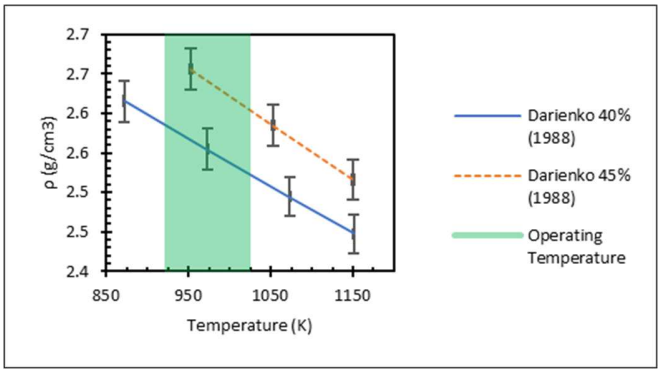

Figure 7 Density as a function of absolute temperature for KF-ZrF_4. Two compositions were analyzed by Darienko et al and assigned approximately 1% error. The resulting correlations can be interpolated to find estimates for the eutectic composition. XX% indicates the percent molar concentration of ZrF_4.

1

2 *Table 3 Coolant salt density data reference.*

Author	Year	Molar Composition (%)	Technique employed	Uncertainty quoted (%)	Temperature Range (K)	No. of Data	Form of Data
			LiF				
Blanke et al.	1956	100	Loss-in-weight Method	1	1096-1268	15	D
Hill et al.	1967	100	Plummet immersion	-	1123-1367	-	E
Jaeger & Khan	1917	100	Hydrostatic weighing	-	887-1058	3	T, E
Mellors & Senderoff	1964	100	Archimedean method	2	1073-1273	3	D
Porter & Meaker	1966	100	Archimedean method	-	1125-1320	31	D
Yaffe & Artsdalen	1956	100	Submerged bob method	-	1149-1320	-	E
			$LiF-BeF_2$				
Blanke et al.	1956	66.67 - 33.33 62.67 - 37.33	Loss-in-weight Method	1	600 - 1175	12 3	D A
Cantor	1973	66 - 34	Nickel dilatometer	0.3	790 - 1100	11	T
			LiF-NaF-KF				
Cheng et al.	2013	46.5 - 11.5 - 42	Archimedean method	0.5	760 - 915	94	D
Cibulkova et al.	2006	46.5 - 11.5 - 42	Archimedean method	-	933 - 1163	-	E
Cohen & Jones	1954	46.5 - 11.5 - 42	Buoyancy principle with plummet	-	873 - 1173	4	E
Mellors & Senderoff	1965	46.5 - 11.5 - 42	Archimedean method	2	940 - 1175	8	D
			$KCl - MgCl_2$				
Grjotheim et al.	1971	67.3263 - 32.6737	Hydrostatic weighing (thermo-vacuum balance)	0.2 - 0.4	1075	1	D
Huber et al	1952	67.25 - 32.75 55.7 - 44.3	Loss-in-weight method, Jolly balance	-	973 - 1173 973 - 1173	3 3	A A
Reding	1965	64.5 - 35.5	Buoyancy method	-	1023 - 1198	-	E
Yuanyuan et al.	2017	68 -32	Archimedean method	-	705 - 1100	9	D
			$KF-ZrF_4$				
Darienko et al.	1988	60 - 40 55 - 45	Maximum gas-bubble pressure	1	872 - 1151 953 - 1150	-	E E

method

$NaF - KF - MgF_2$
N/A

A = averages from data/equation, D = diagram, E = equation, T = tabulated experimental data

Viscosity

Dynamic viscosities are presented in Figure 8-Figure 12 and Table 4 as the majority of the literature presented data in this variable. Any data taken from kinematic viscosity measurements are converted to dynamic viscosity using a relevant density correlation.

LiF: Blanke et al were some of the first to measure LiF's viscosity, doing so with the concentric cylinder method with 5% error [52]. Vetyukov and Sipriya are often cited in data correlations for their work using a torsional pendulum viscometer, but they did not report an error measurement and their data is higher than most other values [69]. Desyatnik et al published two papers in 1979 and 1981 using a damped oscillations method [70], [71], with 2% error in kinematic viscosity for the latter paper. Their data agree well with subsequent measurements (Figure 8). Ejima et al published a comprehensive review of LiF viscosity measurements while taking data of their own with an oscillating cup viscometer at 1-2% error [72]. Abe et al took 58 measurements extending past 1700 K with an oscillating cup viscometer at 0.9% error [73]. Due to the high precision of these measurements with different techniques across several decades, LiF's viscosity appears to be very well defined from 1100-1300 K.

FLiBe: FLiBe has prolific measurement data related to its viscosity; however, contributors investigating its 'recently' discovered 32.8% BeF_2 eutectic are still lacking (Figure 9). The most reliable source is Abe et al [73], who utilized a high temperature oscillating cup viscometer which yielded only 1.3% error. Three series of measurements were used on the same sample cups, but with different specimen wires. Data by Cohen and Jones [74] and Blanke et al [52] fit Abe et al remarkably well. Blanke et al utilized the concentric cylinder method while Cohen & Jones employed both rotational (Brookfield) and capillary viscometers. Cantor [75] published a correlation for 34% BeF_2 with 15% uncertainty, though no measurement method was given.

FLiNaK: Cohen and Jones [76] ran three sets of tests on FLiNaK, one with a modified Brookfield viscometer and the other two by a capillary viscometer as depicted in Figure 10. Cohen et al [77] later cited 10% uncertainty for this experiment. Merzlyakov et al [78] provided the most comprehensive look into FLiNaK's viscosity across a wide range in temperature. Although no uncertainty was cited, Merzlyakov took measurements with torsional oscillation damping from 455 – 870 °C (728 – 1144 K). Measurements made earlier by Vriesema [79] recorded kinematic viscosities with 2% uncertainty using a Venturi flow meter with ceramic insulation for the electrodes on the expansion vessels. Dynamic viscosity was computed using a density equation also listed by Vriesema. Cibulková et al [61], with the oscillatory method (a torsional pendulum), achieving less than 2.5% error. An et al [80] reported values considerably lower than those of Merzlyakov or Cohen, but they align more closely with those of Cibulková. No error was given by An and a modified rotating Brookfield viscometer was used.

KCl-$MgCl_2$: Viscosity for KCl-$MgCl_2$ has been studied solely by Yuanyuan et al [67] per Figure 11. Yuanyuan utilized a high-temperature Brookfield viscometer, which was custom-designed and manufactured by Theta Industrials, Inc. For the eutectic NaCl-KCl-$ZnCl_2$ salt used for calibration, measurement values were within 1% error, but no actual uncertainty was recorded for KCl-$MgCl_2$ data.

FLuZirK: Darienko et al [81] took several viscosity measurements for FluZirK from 0-80% ZrF_4 but unfortunately none at the 42% eutectic composition. However, two compositions with 40 and 50% ZrF_4 were analyzed by a method of damped oscillations. Kinematic viscosity was estimated to have an error of about 2% assuming no pre-calibration was

performed, and dynamic viscosity was then calculated and graphed as shown (Figure 12). Only coefficients to the exponential fit function were recorded. His trends were interpolated by Serrano-López et al [33] to find some agreement with Williams et al [34].

NaF - KF - MgF_2: No available viscosity data was found for this salt.

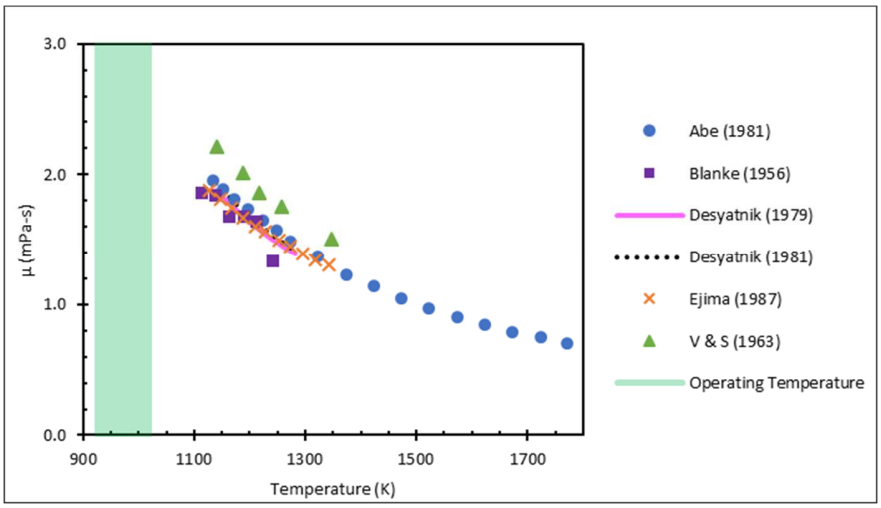

Figure 8 Dynamic viscosity as a function of absolute temperature for LiF. Abe et al reported 0.9% error, Blanke et al reported 5%, Desyatnik et al (1981) reported 2%, and Ejima et al reported 1-2%. Desyatnik et al (1979) and Vetyukov and Sipriya (V & S) did not provide error estimates. Error bars are omitted for clarity.

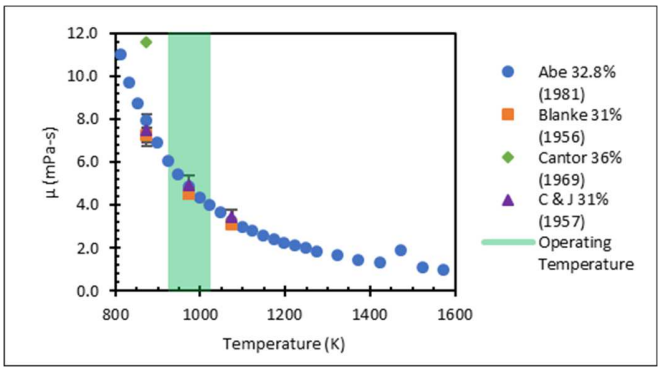

Figure 9 Dynamic viscosity as a function of absolute temperature for FLiBe. XX% indicates the molar percentage of BeF_2 in the sample. Cohen and Jones (C & J) reported 10% error, Blanke reported 5%. Abe et al reported 1.3% error which is omitted for clarity. No error was reported for Cantor's single value.

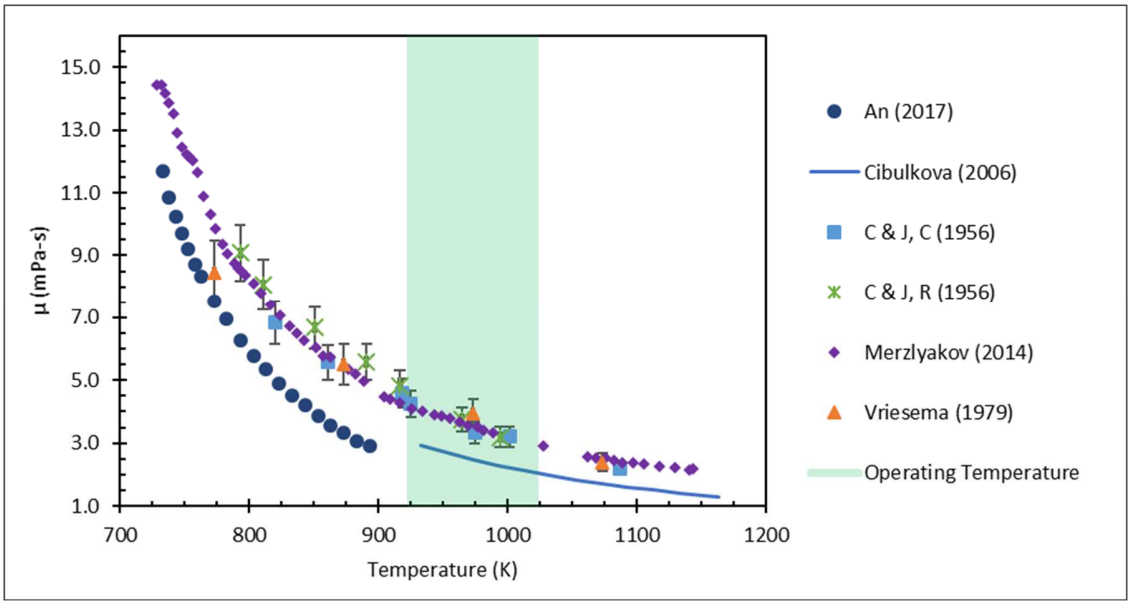

Figure 10 Dynamic viscosity as a function of absolute temperature for FLiNaK. Cibulková et al reported an experimental trend line with < 2.5% error (error not shown). Cohen and Jones (C & J) employed both a capillary (C) and rotational Brookfield (R) viscometer but reported no error. However, a 10% error was later assigned by Cohen et al in 1956 and is displayed. Vriesema reported 2% error for the average kinematic viscosity values reported, and a density correlation with 10% error was used to calculate dynamic viscosity.

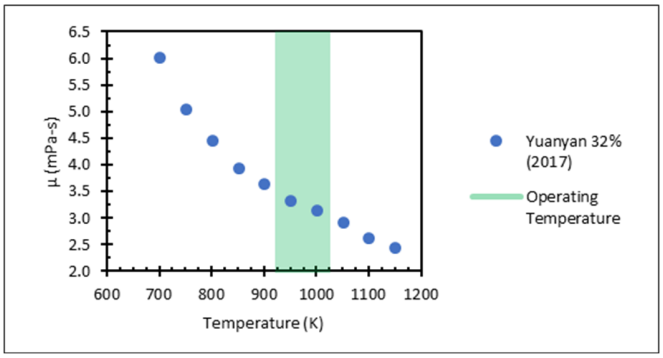

Figure 11 Dynamic viscosity as a function of absolute temperature for KCl-$MgCl_2$. Yuanyuan et al performed the only experimental data for this property, with no error reported. XX% in the legend indicates the percent molar concentration of $MgCl_2$.

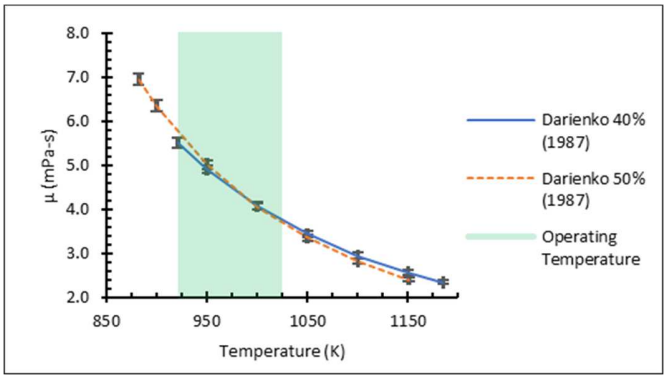

Figure 12 Dynamic viscosity as a function of absolute temperature for KF-ZrF_4. Two compositions were analyzed by Darienko et al and assigned approximately 2% error. The resulting correlations can be interpolated to find estimates for the eutectic composition. XX% indicates the percent molar concentration of ZrF_4.

Table 4 Coolant salt dynamic viscosity data reference.

Author	Year	Molar Composition (%)	Technique employed	Uncertainty quoted (%)	Temperature Range (K)	No. of Data	Form of Data
			LiF				
Abe et al.	1981	100	Oscillating cup viscometer	0.9	1133-1772	58	T
Blanke et al.	1956	100	Concentric cylinder viscometer	5	1114-1241	6	D
Desyatnik et al.	1979	100	Damping of torsional oscillations of a cylinder	-	1139-1282	-	E
Desyatnik et al.	1981	100	Damping of torsional oscillations of a cylinder	~2	1139-1282	-	E
Ejima et al.	1987	100	Oscillating cup viscometer	~1-2	1128-1341	11	T
Vetyukov & Sipriya	1963	100	Torsional pendulum method	-	1140-1348	5	T
			$LiF-BeF_2$				
Abe et al.	1981	67.2 - 32.8	Oscillating cup viscometer	1.3	813 - 1573	96	T
Blanke et al.	1956	69 - 31 62.67 - 37.33	Concentric cylinder viscometer	5	442 - 905	3 6	A D
Cantor	1968	66 - 34	Unpublished measurements	15	-	-	E
Cantor	1969	64 - 36	Brookfield LVT viscometer	-	600	1	D
Cohen & Jones	1957	69 - 31	Capillary and Brookfield viscometer	10	600 - 800	3	A
			LiF-NaF-KF				
An et al.	2017	46.5 - 11.5 - 42	Modified rotating Brookfield viscometer	-	733 - 893	20	T
Cibulkova et al.	2006	46.5 - 11.5 - 42	Torsional pendulum method	< 2.5	933 - 1163	-	E
Cohen & Jones	1956	46.5 - 11.5 - 42	Modified Brookfield rotational device and capillary efflux viscometer	-	793 - 1086	14	D
Merzlyakov et al.	2014	46.5 - 11.5 - 42	Damping of torsional oscillations of a cylinder	-	728 - 1143	58	D
Vriesema	1979	46.5 - 11.5 - 42	Venturi flow meter	2	773 - 1073	4	A
			$KCl - MgCl_2$				
Yuanyuan et al.	2017	68 - 32	Brookfield viscometer	-	700 - 1150	10	D
			$KF-ZrF_4$				

Darienko et al.	1987	60 - 40 50 - 50	Oscillating cup viscometer	~2 (uncalibrated)	921 - 1185 882 - 1151	-	E E
NaF - KF - MgF_2							
N/A							

A = averages from data/equation, D = diagram, E = equation, T = tabulated experimental data

Specific Heat (constant pressure)

Volumetric heat capacity represents one of the most important properties in salt selection [31]. For the same change in temperature and given mass, salt with a larger volumetric heat capacity can move more heat from the reactor to the power plant [31]. This allows for less processing of spent fuel or radiated coolant as well a reduction of heat transfer equipment [31]. Due to the temperature invariance of the data, c_p values are reported as single values in Table 5 with the exception of LiF and FLiNaK, which are presented in Figure 13 and Figure 14.

LiF: Douglas and Dever are commonly cited for their early measurements using an ice calorimeter [35]. However, their measurements only spanned about 80 K past the melting point (Figure 13). They reported 1.5% error. Macleod's data with an adiabatic vacuum drop calorimeter covered a much broader range, but his results are not congruent with the generally acknowledged constant specific heat for liquidus molten salts. Macleod reported heat capacity with an exponential, albeit low, dependence on temperature, though this could be well within his unreported error [82]. The NIST-JANAF thermochemical tables compiled in 1998 reported a constant specific heat up to 2900 K [83].

FLiBe: Rosenthal et al [84] tested two samples of FLiBe in Inconel capsules using separate copper-block drop calorimeters. Sixteen enthalpy measurements yielded 1.4% error across the temperature range, and the value of 0.577 cal/g*K matched the value by Hoffman (reported by Cantor [75]). Douglas and Payne [85] obtained a slightly lower value of 0.561 cal/g*K with an ice Bunsen calorimeter but were working with Li_2BeF_4 compound. This composition approaches that of the FLiBe mixture but had a purity of only 98.6%, which may explain why Douglas and Payne's report yielded considerably more error (3%).

Cantor [75] also reported isochoric specific heats which were calculated from isobaric values, though they are not plotted here.

FLiNaK: Four studies account for the available measurement data on FLiNaK's specific heat (Figure 14). The first by Blalock and Powers [86] cited studies performed at ORNL, National Bureau of Standards (NBS), and Naval Research Laboratory (NRL), but only gave the measurement technique of ORNL (ice calorimeter). However, a copper-block calorimeter was vaguely attributed to another of the sources in the method section. The large change in specific heat around 454 °C (727 K) reflected the melting point of FLiNaK; data for solid mixes are omitted in Figure 14. No error was reported for NRL or NBS, but their heat capacity dropped off linearly with temperature, and further investigation would be needed to explain this result. The second study by Khokhlov et al [87] in 2011 reported well-organized data at temperatures exceeding MSR requirements. Khokhlov employed a STA 449C Jupiter synchronous thermal analyzer (DSC) to produce a data sample with 5% uncertainty. Data under-predicted the trend recorded by Rogers et al [41] employing a Perkin-Elmer DSC-Model 2 calorimeter, but Rogers' composition was not quite eutectic. Rogers reported only 2% error for 23 sample measurements.

KCl-$MgCl_2$: Yuanyuan et al [67] remains the sole retrievable contributor to this salt's heat capacity. Nine measurements with a simultaneous differential scanning calorimetry (DSC) and thermogravimetric analysis system yielded a constant value of 0.239 cal/g*K (0.999 J/g*K) from 704 - 1103 K.

FLuZirK: None exist according to Serrano-López et al [33].

NaF - KF - MgF_2: No available specific heat data was found for this salt.

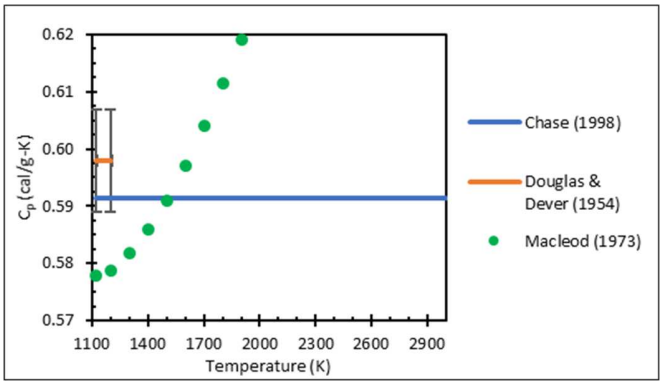

Figure 13 Specific heat capacity (isobaric) as a function of absolute temperature for LiF. Douglas and Dever reported 1.5% error, and both they and Chase noted constant heat capacity. Macleod's values were not temperature independent, but this may be due to his unreported error as he noted 1% agreement with Douglas and Dever's results.

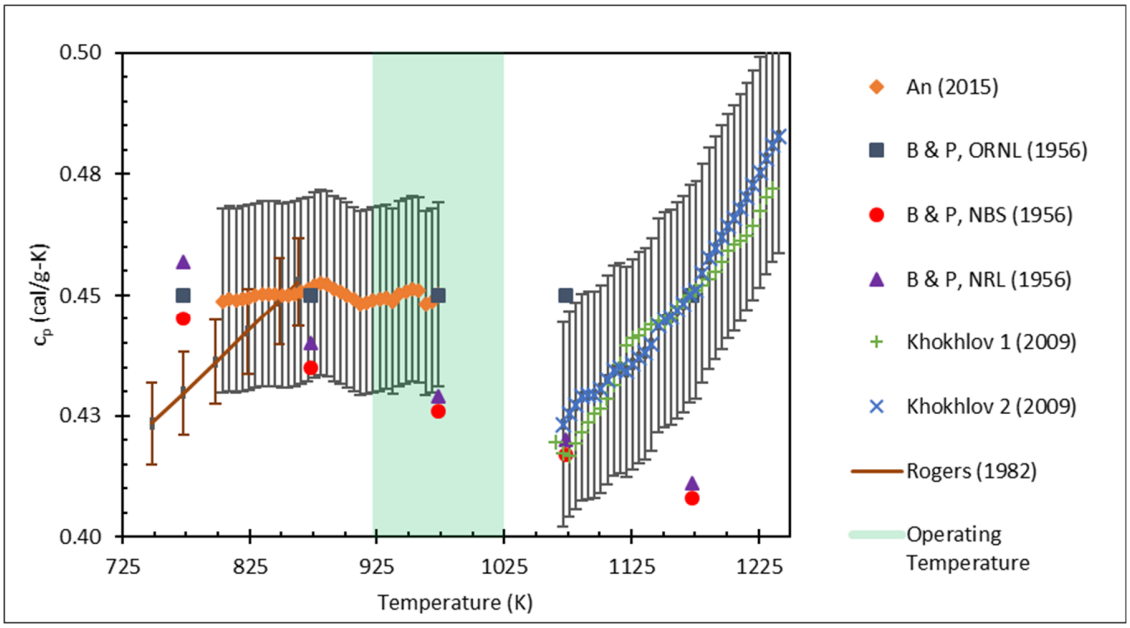

Figure 14 Specific heat capacity (isobaric) as a function of absolute temperature for FliNaK. An et al (An) reported ~4.26% error for their values, which agreed closely with the Blalock and Powers (B &P) test conducted at ORNL. Heat capacity data obtained NBS and NRL differed with a negative temperature dependence. Khokhlov et al's two tests (Khokhlov 'X') reported the opposite, a positive temperature dependence with 5% error. Rogers et al also reported a correlation with a positive temperature dependence over a lower temperature range and only 2% error.

Table 5 Coolant salt specific heat capacity data reference.

Author	Year	Molar Composition (%)	Technique employed	c_p (cal/g*K)	Uncertainty quoted (%)	Temperature Range (K)	No. of Data	Form of Data
			LiF					
Chase	1998	100	-	0.5914	-	1121-3000	1	A
Douglas & Dever	1954	100	Ice Calorimeter	0.5979	1.5	1121 - 1169	1	A
Macleod	1973	100	Adiabatic vacuum drop calorimeter	0.577-0.627	-	1121-2000	10	T
			$LiF-BeF_2$					
Cantor	*1968*	*66 - 34*	*Estimate/ Calculation*	*0.284-0.29*	-	*773 - 973*	*3*	*A*

Douglas & Payne	1969	Li_2BeF_4 (13.85% Li, 9.34% Be, 75.95% F)	Drop method- ice Bunsen calorimeter	0.561	3	745 - 900	8	T
Hoffman & Cooke (Cited by Cantor 1968)	1968	66 - 34	Unpublished measurements at ORNL	0.577	-	-	1	A
Rosenthal et al.	1968	66 - 34	Inconel capsules with 2 copper block drop calorimeters	0.577	1.4	773 - 993	16	D
LiF-NaF-KF								
An et al.	2015	46.5 - 11.5 - 42	ASTM E 1269-11 (DSC)	0.45	4.3	804 - 973	34	D
Blalock & Powers	1956	46.5 - 11.5 - 42	ORNL - Ice calorimeter NBS - ? NRL - ?	See figures	-	373 - 1173 773 - 1173 373 - 1173	9 5 9	A A A
Khokhlov et al.	2009	46.5 - 11.5 - 42	STA 449C Jupiter synchronous thermal analyzer (DSC)	See figures	5	1066 - 1240	70	D
Rogers et al.	1982	46.6 - 11.4 - 42	Perkin-Elmer DSC-Model 2 calorimeter	See figures	2	748 - 863	-	E
KCl - $MgCl_2$								
Yuanyuan et al.	2017	68 - 32	Simultaneous DSC, thermogravimetric analysis	0.24	-	704 - 1103	9	D
KF-ZrF_4								
N/A								
NaF - KF - MgF_2								
N/A								

**Italics* represent isochoric specific heats (c_v).

A = averages from data/equation, D = diagram, E = equation, T = tabulated experimental data

Thermal Conductivity

Thermal conductivity is the key property in determining heat transfer and temperature distribution inside of the salt and plays a critical role in determining heat transfer coefficients from the Nusselt number ($Nu_D = hD/k_f$). It is a difficult parameter to both measure (because of confounding errors introduced by convective and radiative heat transfer modes [88]) and predict [89] from constituent materials. It therefore represents an area where ongoing research is needed, particularly since the trend of most experimental data shows an increase in k as temperature increases (contrary to theoretical predictions) [6]. Data on the thermal conductivity of coolant salts is provided in Figure 15-Figure 18 and Table 6.

LiF: Sreenivasan and Altman [90] sought to measure the thermal diffusivity of molten salts with applications to solar power conversion systems and thermal storage. They employed a "quasi steady state" method where temperature difference was measured across a sample-filled annulus as temperature increased. No error was reported, but Janz [37] estimated it at ±25%. Smirnov et al [91] attempted reduction of radiative heat transfer through a platinum crucible and

zone melting purification of the salts. A maximum error of ±4% was reported, but unfortunately an increase in *k* was noted for increasing temperature. Jaworske and Perry [92] investigated LiF to potentially enhance its liquidus conductivity with graphite fibers. While only taking measurements near 930 °C, they extracted thermal conductivity data from a hot filament heater paired with a DTA via the Van der Held model [93]. More recently, Gheribi et al [89] published a model characterizing the thermal conductivity of molten salts, taking into account radiative effects. Their model is plotted against the above data in Figure 15.

FLiBe: Cooke [94] researched thermal conductivity value corrections and determined that a main cause of historic error was heat shunting. Modifications were made to an absolute, variable-gap apparatus using fluids to minimize thermal resistance in the measured temperature range. The results were applied to FLiBe, with a maximum error of 15%. Rosenthal et al. [84] followed a similar pattern by using an absolute, variable-gap apparatus, noting corrections to be made for radial heat transfer, natural circulation, and radiation. Their error estimates were 15-35%, with the more conservative value being shown in Figure 16. It should be noted that Cantor [75] presents a value of 1.0 W/m*K with an error of ± 10%. The method to obtain this value was irretrievable but apparently available in the Proceedings of the Sixth Conference on Thermal Conductivity as cited in his work. This value is not temperature dependent; Cantor argued that variation with temperature was masked by current measurement uncertainty, and thus not documented. Results are shown in Figure 16.

FLiNaK: Cooper and Claiborne [95] experimented on the thermal conductivity of FLiNaK using a Deem type apparatus (parallel plate method), which was a heated salt bath with thermocouples placed slightly below in the sample wall. Three independent measurements were taken on two segments of the container with a maximum error of ±13.8%. Ewing et al [96] ran three experiments in 1962, where he primarily accounted for variation due to impurities. With each test, he noted that radiative heat transfer decreased due to increasing amounts of chromium in his uniaxial apparatus. Khokhlov et al [87] and Smirnov et al [91] differed drastically from previous experimental results. As noted for LiF, Smirnov et al sought reduction of radiative heat transfer via a platinum crucible and zone melting purification of the salts with ±4% error reported. Khokhlov et al used steady-state nickel coaxial cylinders and were laborious in their attempts to reduce non-conductive heat transfer. Ueki et al reported a single value using the transient hot-wire method with ±4.1% error [97]. Most recently, An et al [98] calculated thermal conductivity using thermal diffusivity measured with the laser flash technique. Values for density were taken from Cheng et al [62] and specific heat was performed by DSC as discussed in the previous section. A custom graphite crucible had been designed and calibrated with both water and KNO_3 to ensure reliable results, and An's work agrees well with both Khokhlov and Smirnov (Figure 17).

KCl-$MgCl_2$: Polyakov and Gildebrandt [99] performed a study of this salt using the coaxial cylinder method (Figure 18). Calibrating with both water and KNO_3, results agreed within 2% and 8%, respectively, of accepted values. They estimated their results for the chloride salt to be within ±10%. Polyakov and Gildebrandt also offered commentary on why there was a positive temperature coefficient for fused salts when covalently bonded salts had the opposite. They recommended investigation into the phonon mechanism of heat transfer. This is in contrast to the negative temperature dependence considered valid for chloride salts as discussed by Assael et al [6]. Yuanyuan et al [67] cited a correlation of thermal conductivity published by Janz and Tomkins [42], which is based on the work of Polyakov and another irretrievable source.

FLuZirK: According to Serrano-López et al [33], no thermal conductivity data exists for this salt.

NaF - KF - MgF_2: No available thermal conductivity data was found for this salt.

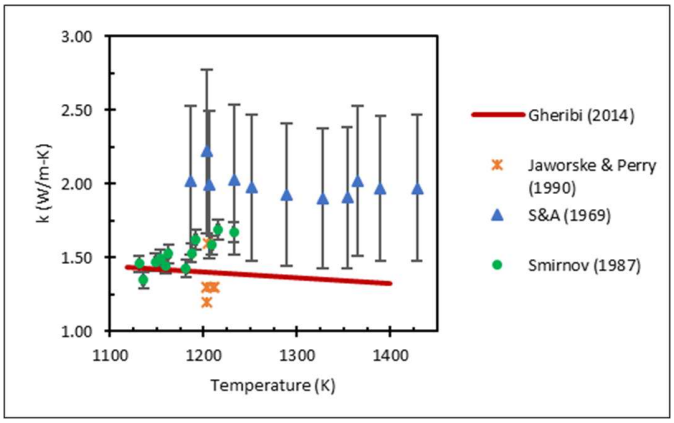

Figure 15 Thermal conductivity as a function of absolute temperature for LiF. Sreenivasan & Altman (S&A) did not directly report an uncertainty estimate, but Janz 1979 estimated it at 25%. Smirnov et al. reported an error of 4%. Gheribi et al. and Jaworske and Perry provided no error estimates.

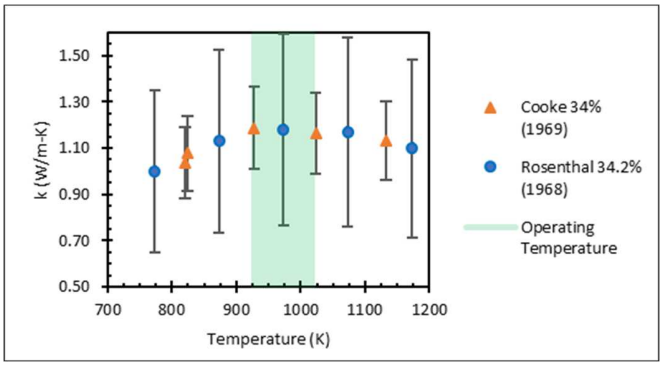

Figure 16 Thermal conductivity as a function of absolute temperature for FLiBe. XX% represents the % molar concentration of BeF_2 in each sample. Rosenthal et al reported 15-35% error (35% shown) while Cooke reported a maximum error of 15% (15% shown). Rosenthal's values were likely evaluated from a correlation which was not presented.

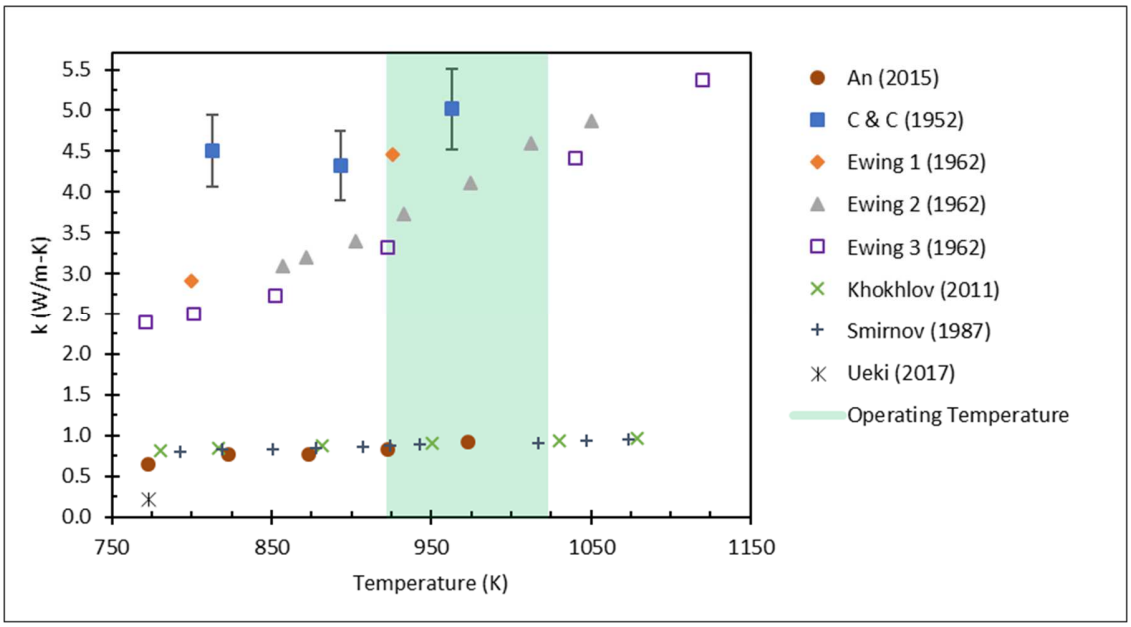

Figure 17 Thermal conductivity as a function of absolute temperature for FLiNaK. Cooper and Claiborne (C & C) and Ewing et al's three tests (Ewing X) appear highly skewed due to convective and radiative error. Recently, Khokhlov et al, Smirnov et al, Ueki et al, and An et al have published data which agree reasonably well with each other. Error for each: 8-14% (C&C, 9.8% displayed), 4% (Smirnov et al), 2.5-3.5% (An et al), 4.1% (Ueki et al) and <4% (Khokhlov et al). All but Cooper and Claiborne do not have error displayed for clarity.

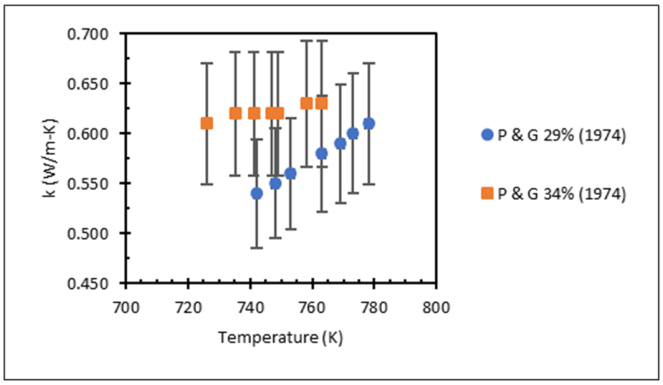

Figure 18 Thermal conductivity as a function of absolute temperature for KCl-$MgCl_2$. XX% indicates the percent molar concentration of $MgCl_2$ in the sample. Polyakov and Gildebrandt (P & G) tested two compositions which can be interpolated for the eutectic. An error of 10% was reported. No values were taken approaching MSR operating temperature.

Table 6 Coolant salt thermal conductivity data reference.

Author	Year	Molar Composition (%)	Technique employed	Uncertainty quoted (%)	Temperature Range (K)	No. of Data	Form of Data
			LiF				
Gheribi et al.	2014	100	Model	-	1118-1400	-	E
Jaworske & Perry	1990	100	Hot filament technique	-	1204-1210	6	T
Sreenivasan & Altman	1969	100	Quasi-steady state cylinder method	25	1186-1428	11	D
Smirnov et al	1987	100	Platinum coaxial cylinders	4	1131-1232	12	D
			$LiF-BeF_2$				
Cantor (Unpublished measurements by Cooke at ORNL)	1968	66 - 34	p. 15 in Proceedings of the Sixth Conference on Thermal Conductivity, Dayton, Ohio, Oct. 19-21, 1966.	10	-	1	A
Cooke	1969	66 - 34	Absolute variable gap apparatus	-	820 - 1133	5	D
Rosenthal et al.	1968	63.8 - 34.2	Absolute variable gap apparatus	15 - 35	773 - 1173	5	A
			LiF-NaF-KF				
An et al.	2015	46.5 - 11.5 - 42	Laser Flash	2.5 - 3.5	773 - 973	5	T
Cooper & Claiborne	1952	46.5 - 11.5 - 42	Deem type apparatus	7.7 - 13.8	763 - 1020	3	A
Ewing et al.	1962	46.5 - 11.5 - 42 (increasing impurities in each test)	Uniaxial Inconel apparatus	-	800 - 1120	15	D
Khokhlov et al.	2011	46.5 - 11.5 - 42	Steady state nickel coaxial cylinders	< 4	780 - 1080	6	D

Smirnov & Khokhlov	1986	Eutectic	Platinum coaxial cylinders	< 4	792 - 1074	10	D
Ueki et al	2017	46.5 - 11.5 - 42	Transient hot-wire	4.1	773	1	T
$KCl - MgCl_2$							
Polyakov & Gildebrandt	1974	71 - 29 66 - 34	Coaxial cylinder with graphite cell	10	742 - 778 726 - 763	7 7	T T
$KF-ZrF_4$							
N/A							
$NaF - KF - MgF_2$							
N/A							

A = averages from data/equation, D = diagram, E = equation, T = tabulated experimental data

Electrical Conductivity

Simply put, the electrical conductivity of a substance represents the limiting value of the current density over the electrical field strength at low frequencies [100]. It is the reciprocal of the cell resistance multiplied by the cell constant [101]. Electrical conductivity allows for the structure and transport theory of molten salts to be characterized. Current and electrolytic efficiencies necessitate conductivity values in order to be calculated [102]. In addition, design of electrical circuits and potentially the mass transfer of fluoride systems are affected by this property.

One difficulty that can arise in measuring thermophysical properties of salt is the ability of the salt to conduct electricity. This is particularly problematic when measuring thermal conductivity by the transient hot wire technique, which is used by NIST to establish reference data for liquids [103]. Figure 19-Figure 22 and Table 7 present electrical conductivity values for coolant salts.

LiF: Electrical conductivity was one of the most thoroughly investigated properties for LiF (Figure 19). Yaffe and Artsdalen [51] applied a then recently developed low resistance transformer bridge and improved cell design for more corrosive fluoride salts. Calibration with KCl yielded highly reproducible results, though no error was evaluated for LiF specifically. The following year, Yim and Feinleib [104] published conductivity values for cryolites, having recently developed a boron nitride cell with Inconel electrodes for high temperature stability [105]. Empty cell resistance was their largest source of error, but standard deviation remained within 0.3-1.4%. Winterhager and Werner used platinum electrodes with a wheatstone bridge [106]. Brown and Porter [107] measured LiF paired with UF_4 and ThF_4 using a graphite lined boron nitride cell to prevent cell resistance changes. With molybdenum electrodes, they matched Yaffe and Artsdalen's calibration data within ±0.4%. Matiasovsky et al [108], [109] instead used all platinum cells and electrodes with high agreement to Yim and Feinleib. Matiasovsky's 1970 report cited 2% error, and this is likely a good estimate for the latter work with the same method. Danek et al's method was likely with a platinum cell as well [110]. Balakir et al used Kohlrausch's law and a platinum cell measurement technique [111], but their data was much lower than the rest in this set and is not displayed in the figure below for clarity.

FLiBe: Two studies by Braunstein and Robbins provide most of the knowledge of FLiBe's electrical conductivity (Figure 20). All compositions were taken at 34% BeF_2 and incorporated some form of silica cell with a Wheatstone bridge. Both studies were performed by these authors and will be distinguished instead by ORNL paper number. ORNL-4254 [112] estimated an uncertainty of electrical conductivity < 10%. ORNL-4449 [113] improved upon the former study with an AC-Wheatstone bridge and enhanced silica cell, with temperatures taken over a broader range. The bridge contained a variable resistor and capacitor in series. As a result, error was markedly reduced and estimated at ±0.5%. A comprehensive summary of FLiBe's electrical conductivity data across multiple compositions is presented in ORNL-4548 [114].

FLiNaK: Greene [115] is the only known source for electrical conductivity values on FLiNaK (Figure 21). As his calibrated apparatus was within 10% error of known salts, he estimated a similar uncertainty for the fluoride sample tested.

Greene utilized a current-potential conductivity cell where current and voltage measurements were taken separately to mitigate polarization effects.

KCl-$MgCl_2$: Huber et al [66] examined KCl-$MgCl_2$ using a fused silica conductivity cell, being the only known source for electrical conductivity values near eutectic compositions (Figure 22). No uncertainty was recorded, but a clear linear trend was exhibited.

FLuZirK: No available electrical conductivity data was found for this salt.

NaF - KF - MgF_2: No available electrical conductivity data was found for this salt.

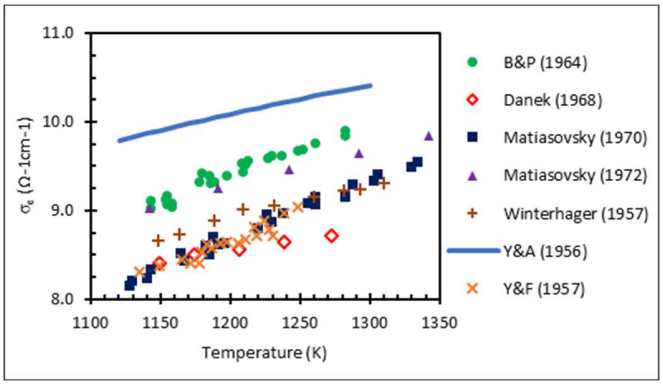

Figure 19 Electrical conductivity as a function of absolute temperature for LiF. Brown and Porter (B&P), Danek, Yaffe and Artsdalen (Y&A), and Yim and Feinleib (Y&F) did not report error estimates for their values but noted high reproducibility and agreement with their calibration salts. Matiasovsky et al (1970) noted 2% error (not displayed for clarity), which could reasonably be applied to their 1972 values given the similarities of experiment.

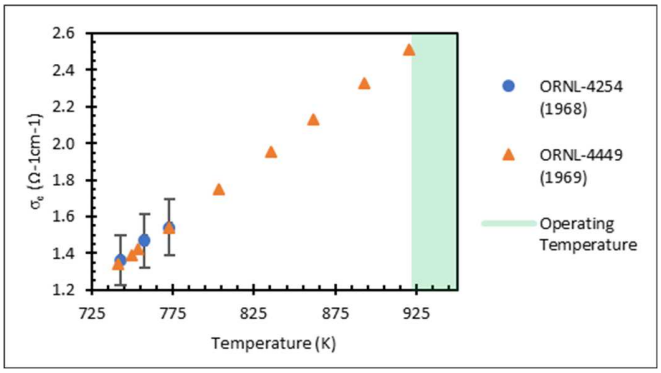

Figure 20 Electrical conductivity as a function of absolute temperature for FLiBe. Together, Braunstein and Robbins conducted two studies (ORNL-4254 and ORNL-4449) using silica conductivity cells. ORNL-4254 reported <10% error (10% shown) and ORNL-4449 reported 0.5% error, which was not shown for clarity. Both samples possessed a 34% molar composition of BeF_2. Note that both studies were conducted below MSR operating temperature.

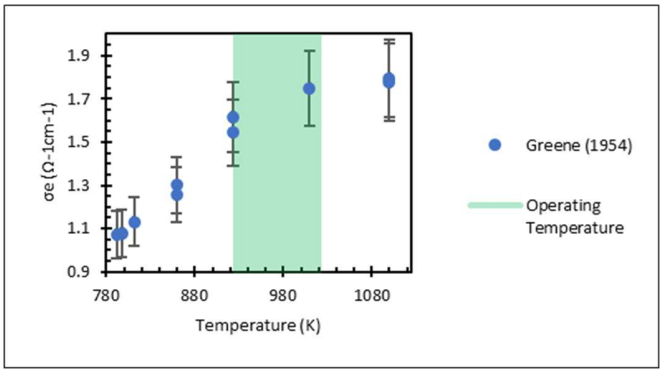

Figure 21 Electrical conductivity as a function of absolute temperature for FLiNaK. Greene is the only source of measurement for this property, with 10% error being reported. The flattening of data after 980 K necessitates more research into this property for the eutectic composition.

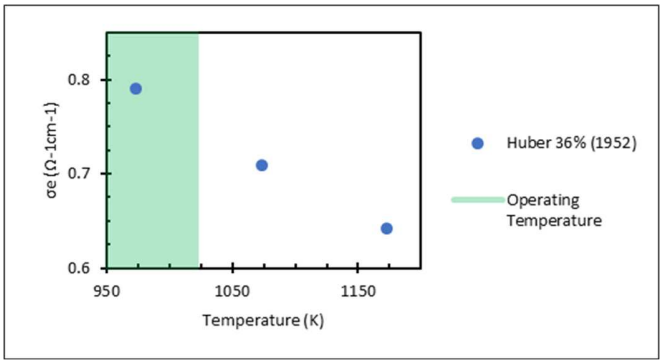

Figure 22 Electrical conductivity as a function of absolute temperature for KCl-$MgCl_2$. XX.X% indicates the percent molar concentration of $MgCl_2$. No work presented error except Huber et al, with no error reported.

Table 7 Coolant salt electrical conductivity data reference.

Author	Year	Molar Composition (%)	Technique employed	Uncertainty quoted (%)	Temperature Range (K)	No. of Data	Form of Data
			LiF				
Balakir et al.	1968	100	Kohlrausch method with Wheatstone bridge and platinum cell	-	1173-1573	5	A
Brown & Porter	1964	100	Boron nitride cell w/ graphite jackets, Mo electrodes.	-	1142-1282	25	D
Danek et al.	1968	100	Likely a platinum cell design.	-	1148-1272	5	D
Matiasovsky et al.	1970	100	Platinum cell and electrodes, Thompson bridge.	-	1127-1334	24	D
Matiasovsky et al.	1972	100	All platinum cell and electrodes	2	1141-1342	5	D

Winterhager & Werner	1957	100	Platinum electrodes and wheatstone bridge	-	1148-1310	9	T
Yaffe & Artsdalen	1956	100	Transformer bridge, precious metal electrodes	-	1120-1300	-	E
Yim & Feinleib	1957	100	Boron nitride cell, inconel electrodes	-	1135-1248	19	D
			$LiF-BeF_2$				
Braunstein & Robbins	1968	66 - 34	Silica cell with Wheatstone bridge	< 10	745 - 775	3	D
Braunstein & Robbins	1969	66-34	Silica cell with AC Wheatstone bridge	0.5	741 - 920	9	T
			LiF-NaF-KF				
Greene	1954	46.5 - 11.5 - 42	Current potential conductivity cell	-	792 - 1100	10	D
			$KCl - MgCl_2$				
Huber et al	1952	66 - 34	Fused silica conductivity cell	-	973 - 1173	3	D
			$KF-ZrF_4$				
			N/A				
			$NaF - KF - MgF_2$				
			N/A				

A = averages from data/equation, D = diagram, E = equation, T = tabulated experimental data

3. Investigation of Fueled Salt Properties

This section details the existing thermophysical properties from literature for the candidate salts in Section 1 containing fuel (where available). The only candidate salts containing uranium or thorium-based fuel in this review are FLiBe and FLiNaK. The discussion of properties will be similar to coolant salts from Section 2. Properties include: melting point and at specific molar compositions, density (ρ), viscosity (μ, ν), specific heat and constant pressure (c_p), thermal conductivity (k), and electrical conductivity (σ_e).

Melting Point

Table 8 presents melting point and molar compositions for salts containing ThF_4, UF_4, or both.

$LiF-BeF_2-ThF_4$: Thoma et al [116] reported a single ternary eutectic at 1.5% ThF_4. Six sets of quenching and temperature measurements were made, each employing 18 thermocouples. The 1.7% error in invariant temperature measurements depended largely upon the accuracy of the chromel-alumel thermocouples. Capelli [117] optimized his quasi-chemical model based upon Thoma's experimental results, and his lowest ternary melting point matched well with Thoma's work. Van der Meer et al [118] extracted Thoma's data and calculated precipitation temperatures using the Equilib module in FactSage. However, correlations with DTA and thermal quenching varied not just in melting point but in composition and van der Meer's model-based eutectic value is off by nearly 70 K from Thoma's experimentation.

LiF-BeF_2-UF_4: Listed as "mixture 75" by Cohen et al [77], Cohen cited a melting temperature for FLiBe uranium with an unknown method. Capelli [117] found just two eutectics, both with extremely high concentrations of BeF_2, which would likely lead to highly viscous, glassy compositions. Van der Meer [118] again compared his LiF-BeF_2-UF_4 models with experimental data, and found similar errors as with the thorium ternaries when they were measured using DTA or quenching. Van der Meer recommended reevaluating the compositions with DTA, and if a genuine difference remained, to reassess their model. However, the most comprehensive study to date was performed by Jones et al [28] using three different measurement techniques (DTA, thermal gradients, and filtration). Two low temperature eutectics were found.

LiF-BeF_2-ThF_4-UF_4: Four compositions followed by Cantor [75] were assigned melting temperatures with 1% error, though no measurement procedure was recorded. These values may have been recorded from MSRE trials. Cohen et al [77] assigned a similar molar composition one of the melting temperatures that Cantor provided. Van der Meer et al followed the experimental values put forth by Cantor to provide model-based values, which over predict respective melting points by 15-20 K (experimental value in Table 8 is in parentheses).

LiF-NaF-KF-ThF_4: No studies have any record of LiF-NaF-KF-ThF_4's melting point, but Cohen et al [77] does present one estimate.

LiF-NaF-KF-UF_4: Cohen et al [77] gives two compositional melting point estimates and also cites Cisar for an experimental value, but this paper is not yet retrievable.

Table 8 Fuel salt melting point data reference.

Author	Year	Molar Composition (%)	Technique employed	Uncertainty quoted (%)	Melting Point (K)
		LiF - BeF_2 - ThF_4			
Capelli	2016	47.5-50.7-1.8	Calculated	-	632.2
Thoma et al.	1960	47 - 51.5 - 1.5	Thermal gradient quenching	1.7	629
van der Meer et al.	2006	48 - 51.5 - 0.5 70 - 24 - 6	Quasi-chemical model	-	695.00 758.90
		LiF-BeF_2-UF_4			
Capelli	2016	8.35-68.68-22.98 1.12-47.9-50.99	Calculated	-	708.1 633.9
Cohen et al.	1956	67 - 30.5 - 2.5	-	-	737
Jones et al.	1962	69 - 23 - 8 48 - 51.5 - 0.5	Differential thermal analysis, thermal gradient quenching, filtration	-	699 623
van der Meer et al.	2006	70 - 12 - 18 49 - 50 - 1	Quasi-chemical model	-	712.90 695.00
		LiF - BeF_2 - ThF_4 - UF_4			
Cantor	1968	73 - 16 - 10.7 - 0.3 72 - 21 - 6.7 - 0.3 68 - 20 - 11.7 - 0.3 63 - 25 - 11.7 - 0.3	-	1	773 773 753 773
Cohen et al.	1956	71 - 16 - 12 - 1	-	-	773
van der Meer et al.	2006	71.7 - 16 - 12 - 0.3	Quasi-chemical model	-	794.5 (773)*
		LiF-NaF-KF-ThF_4			

Cohen et al.	1956	46.2 - 11.4 - 41.8 - 0.6	Estimate	-	723
		$LiF-NaF-KF-UF_4$			
Cohen et al.	1956	44.5 - 10.9 - 43.5 - 1.1	Cisar, J., ORNL CF 51-11-198.	-	725
Cohen et al.	1956	44.7 - 11.0 - 40.3 - 4.0 45.3 - 11.2 - 41.0 - 2.5	Estimate/calculation	-	883 763

* Temperature in '( )' corresponds to experimental value, not the model

Density

Figure 23-Figure 24 and Table 9 present density measurements for salts containing ThF_4, UF_4, or both.

$LiF-BeF_2-ThF_4$: Cantor [57] is the sole author of density data for FLiBe-Thorium fuel (Figure 23). He employed a nickel dilatometer [119] which detected changes in liquid level (while preventing evaporative escape), which initially read an open circuit but then changed to a measured resistance. While most values were taken significantly lower than MSR operating temperature, clear linear trends were shown for each composition. Cantor achieved accuracy within ±0.15% of Archimedean methods while evaluating KNO_3, and total error for the fluoride-based fuel is estimated at ±0.3%.

$LiF-BeF_2-UF_4$: Blanke et al [52] is the only known publisher of measured FLiBe-Uranium density values (Figure 24). The mole fraction reported, 70-10-20% ThF_4 is likely not eutectic. The Archimedean method employing a platinum cylinder was the same method as described previously by Blanke for the FLiBe coolant, and an error of ±1% was given. Much more data will be needed for this mixture at a verified eutectic.

$LiF-BeF_2-ThF_4-UF_4$: Cantor [75] gave four correlations based on four estimates by additivity of molar volume, for which he assigned a 3% uncertainty. Cohen et al. [77] gave a correlation of unspecified temperature range with ±5% uncertainty.

$LiF-NaF-KF-ThF_4$: No experimentally measured density values have been taken for FLiNaK-Thorium. However, Cohen et al [77] published a calculated equation of the 46.2-11.4-41.8-0.6% composition. He estimated a density of 1.8-2.2 g/cm^3 an error of ±5% in his model.

$LiF-NaF-KF-UF_4$: Three compositions were presented by Cohen et al [77]. The first, 44.5-10.9-43.5-1.1 % molar composition is based on work by Cisar with a density of 1.8-2.25 g/cm^3 and 5% uncertainty, but that work has been irretrievable thus far. Two other samples, with 4.0% and 2.5% UF_4, had density correlations presented with equal uncertainty as they were both calculated. Their density values were slightly higher than that obtained by Cisar.

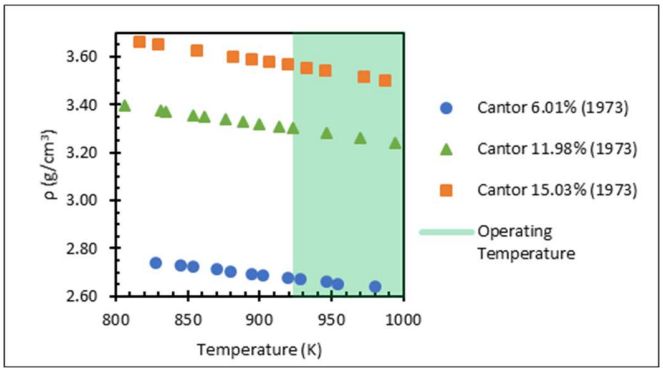

Figure 23 Density as a function of absolute temperature for $LiF-BeF_2-ThF_4$. Analysis yielded a total error of 0.3% which was omitted for clarity. X.XX% indicates the percentage of ThF_4 in each composition.

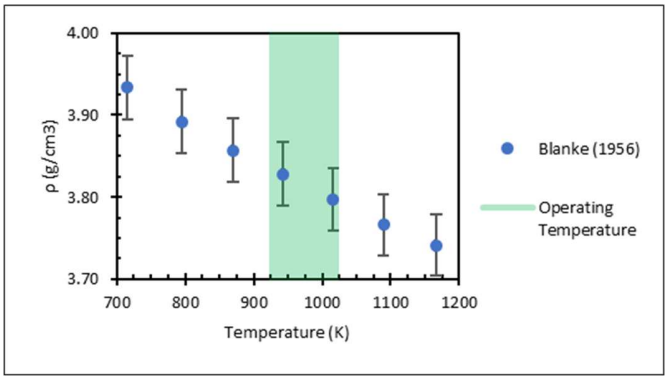

Figure 24 Density as a function of absolute temperature for LiF-BeF_2-UF_4. The composition analyzed by Blanke et al. was not a eutectic composition. An error of 1% was reported.

Table 9 Fuel salt density data reference.

Author	Year	Molar Composition (%)	Technique employed	Uncertainty quoted (%)	Temperature Range (K)	No. of Data	Form of Data
			LiF - BeF_2 - ThF_4				
Cantor	1973	70.11 - 23.88 - 6.01 70.06 - 17.96 - 11.98 69.98 - 14.99 - 15.03	Nickel dilatometer	0.3	830 - 980 806 - 1015 817 - 1023	12 14 13	T
			LiF-BeF_2-UF_4				
Blanke et al.	1956	70 - 10 - 20	'Loss-in-weight' method	1	715 - 1165	7	D
			LiF - BeF_2 - ThF_4 - UF_4				
Cantor	1968	73 - 16 - 10.7 - 0.3 72 - 21 - 6.7 - 0.3 68 - 20 - 11.7 - 0.3 63 - 25 - 11.7 - 0.3	Calculated by additivity of molar volumes	3	-	-	E
Cohen et al.	1956	71 - 16 - 12 - 1	Estimate/ calculation	5	-	-	E
			LiF-NaF-KF-ThF_4				
Cohen et al.	1956	46.2 - 11.4 - 41.8 - 0.6	Estimate/ calculation	5	-	-	E
			LiF-NaF-KF-UF_4				
Cohen et al.	1956	44.5 - 10.9 - 43.5 - 1.1	Cisar, J., ORNL CF 51-11-198.	5	-	-	E
Cohen et al.	1956	44.7 - 11.0 - 40.3 - 4.0 45.3 - 11.2 - 41.0 - 2.5	Estimate/ calculation	5	-	-	E

A = averages from data/equation, D = diagram, E = equation, T = tabulated experimental data

Viscosity

Figure 25-Figure 28 and Table 10 present viscosity measurements for salts containing ThF_4, UF_4, or both.

LiF-BeF_2-ThF_4: Cantor [57] revisited the same compositions of his density tests, but viscosity tests were conducted at Mound Laboratory using an oscillating cup viscometer (Figure 25). This oscillatory method was chosen given the nature

of the volatile and non-viscous salts measured. Three values were taken at each measured temperature, though no uncertainty was reported. Cantor noted that substitution of ThF_4 for BeF_2 caused an increased viscosity for salts composed of 60% LiF or higher. Analogous results were seen for salts containing UF_4 instead of ThF_4 [75].

LiF-BeF_2-UF_4: Multiple ORNL progress reports in the late 1950s were published documenting the viscosity of FLiBe-Uranium, and the abundance of available data are uncharacteristic of this fuel study (Figure 26). Two papers summarizing the results are presented here. ORNL-2684 [120] tested 62-37-1% UF_4 with a modified efflux cup viscometer. Multiple tests were run using this method with the machine being calibrated either with a glycerin-water solution or a ternary nitrate salt. The ternary salt possessed a kinematic viscosity in the same range as the fluoride salt between 500-800 °C. Nitrate tests were run using a viscometer with a serrated skirt which prevented drainage mixing, though the glycerin tests were not modified in this way. Two more tests were run with 70-10-20% composition in ORNL-2723 [121]. Per ORNL-2723, two different labs (ORNL and Mound) tested a Margules design viscometer consisting of two concentric Inconel cylinders. However, some data presented by Mound and referencing Blanke et al's documentation [52] could not be recovered, so they were extracted directly from the chart. Macpherson did not comment on the discrepancy in viscosity obtained by the two labs.

LiF-BeF_2-ThF_4-UF_4: Cantor [75] again presented estimated correlations, although these correlations are based upon estimates from FLiBe-U and FLiBe-Th measurements by Blanke et al [52] and ORNL-2890 [122]. However, the high 25% uncertainty renders the correlations almost inutile. Cohen et al [77] presented three average values from 600-800 °C for 71 LiF-16 BeF_2-12 ThF_4-1 UF_4% based upon experimental (but unpublished) data with 10% error. ORNL-2890 [122] presented the largest accumulation of data for this quaternary salt. A skirted capillary efflux viscometer like the one in ORNL-2684 [120] was used, and therefore likely calibrated with the nitrate salt. No error was given for these measurements. "Salt 134" (62-36.5-1-0.5%) was compared with this investigated mixture, but no source for its viscosity could be found (Figure 27).

LiF-NaF-KF-ThF_4: Average value viscosity estimates at 100 °C intervals for 46.2 LiF-11.4 NaF-41.8 KF-0.6 ThF_4% were presented by Cohen et al [77].

LiF-NaF-KF-UF_4: Cohen et al [77] presented 3 compositions of FLiNaK-Uranium coolant. The first, 44.7-11.0-40.3-4.0% was merely an estimate/calculation listed with 20% error. The other two compositions listed are averages are based on previous measurements from Cohen and Jones [76]. Both compositions were measured using both a modified Brookfield and capillary viscometer. Details or commentary regarding the experimental procedure were not given, nor was the error. However, Cohen et al [77] listed both experiments with 10% error, and this is shown in Figure 28.

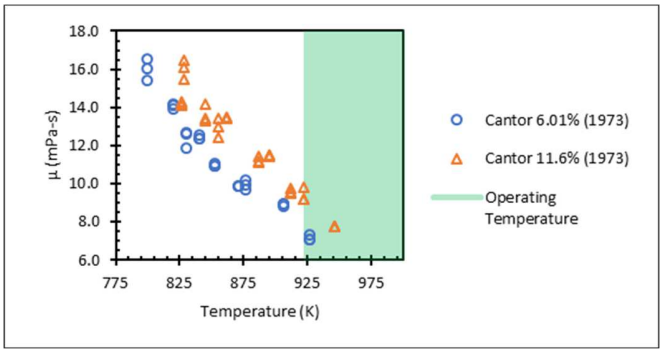

Figure 25 Dynamic viscosity as a function of absolute temperature for LiF-BeF_2-ThF_4. The data appears relatively linear, though the figure represents only a single study. X.XX% indicates the percentage of ThF_4 in each composition.

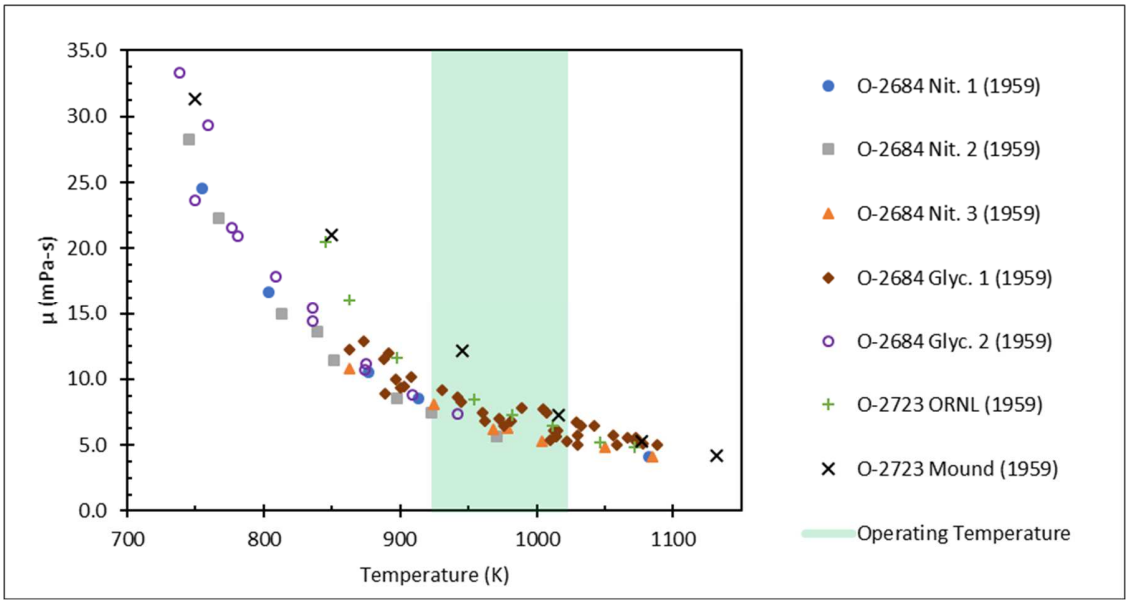

Figure 26 Dynamic viscosity as a function of absolute temperature for LiF- BeF_2-UF_4. MacPherson (ORNL-2684, displayed as O-2684) ran five tests, calibrating either with nitrate salt (Nit) or a glycerine-water solution (Glyc). MacPherson (ORNL-2723, displayed as O-2723) reports data from two separate laboratory experiments. No error was reported, though percent molar concentration of UF_4 ranged from 1-20%.

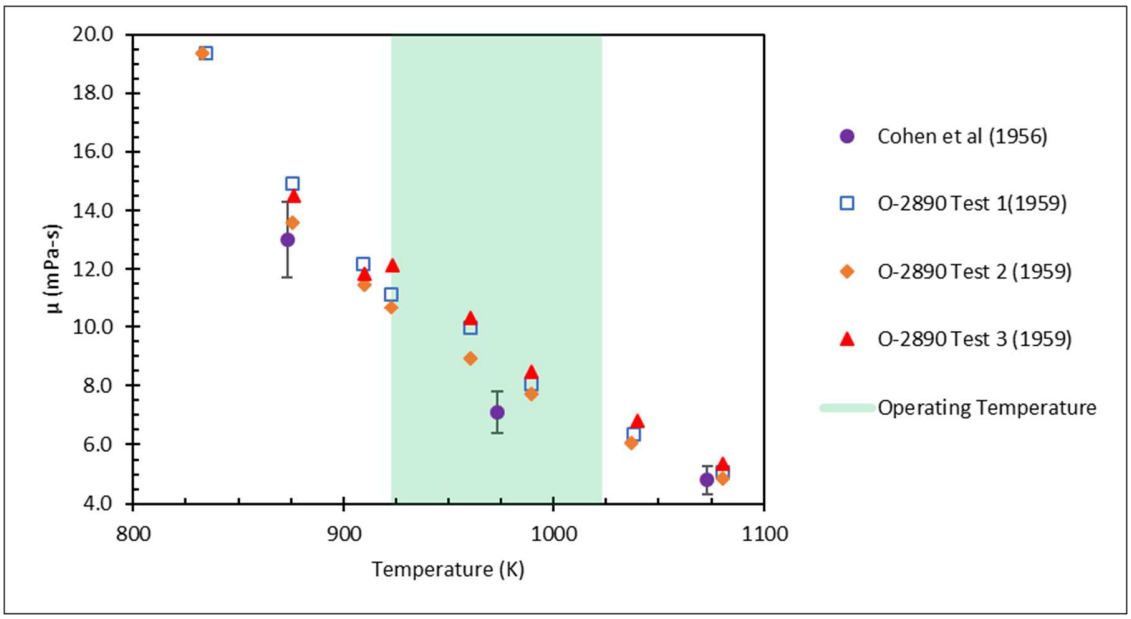

Figure 27 Dynamic viscosity as a function of absolute temperature for LiF- BeF_2-ThF_4-UF_4. Three tests were conducted by MacPherson with strong similarity (O-2890 Test X) while Cohen et al. reported experimental but unpublished values with an error of 10%.

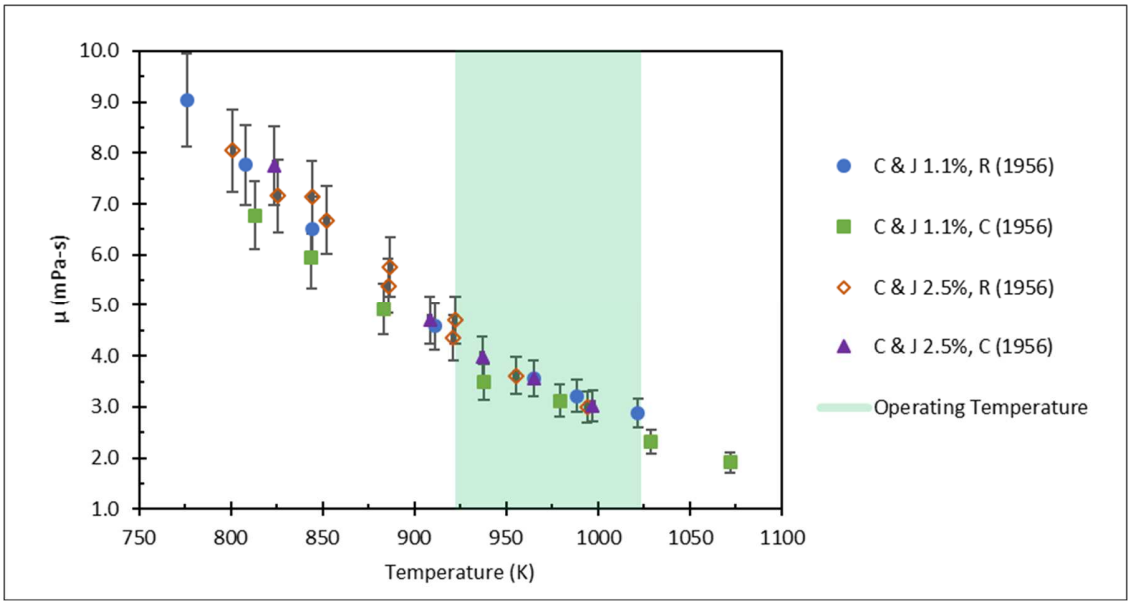

Figure 28 Dynamic viscosity as a function of absolute temperature for LiF-NaF-KF-UF_4. Cohen and Jones (C & J) conducted all tests for this salt with either a rotational Brookfield (R) or capillary (C) viscometer. X.X% indicates the percent molar concentration of UF_4. All samples possessed 10% error.

Table 10 Fuel salt viscosity data reference.

Author	Year	Molar Composition (%)	Technique employed	Uncertainty quoted (%)	Temperature Range (K)	No. of Data	Form of Data
			LiF - BeF_2 - ThF_4				
Cantor	1973	70.11 - 23.88 - 6.01 72.7 - 15.7 - 11.6	Oscillating cup viscometer	-	830 - 925 826 - 946	27 30	T
			LiF-BeF_2-UF_4				
ORNL - 2684	1959	62 - 37 - 1	Modified efflux cup viscometer - Calibrated with various fluids	-	740 - 1090	69	D
ORNL - 2723	1959	70-10-20	Margules design viscometer, two concentric Inconel cylinders	-	750 - 1130	14	D
			LiF - BeF_2 - ThF_4 - UF_4				
Cantor	1968	73 - 16 - 10.7 - 0.3 72 - 21 - 6.7 - .3 68 - 20 - 11.7 - .3 63 - 25 - 11.7 - .3	Estimated by Blanke et al. and ORNL-2890 data	25	-	-	E
Cohen et al.	1956	71 - 16 - 12 - 1	Unpublished data	10	873 - 1073	3	A
ORNL 2890	1959	67 - 18.5 - 14 - .5	Skirted capillary efflux viscometer	-	833 - 1081	23	D
			LiF-NaF-KF-ThF_4				
Cohen et al.	1956	46.2 - 11.4 - 41.8 - .6	Estimate/ calculation	-	775 - 1075	4	A
			LiF-NaF-KF-UF_4				

Cohen and Jones	1956	44.5 - 10.9 - 43.5 - 1.1 45.3 - 11.2 - 41.0 - 2.5	Modified Brookfield viscometer and capillary viscometer	10*	776 - 1135 801 - 997	15 15	D
Cohen et al.	1956	44.7 - 11.0 - 40.3 - 4.0	Estimate/ calculation	20	873 - 1073	3	A

*Uncertainty recommended by Cohen et al (1956).

A = averages from data/equation, D = diagram, E = equation, T = tabulated experimental data

Specific Heat (constant pressure)

Table 11 presents specific heat measurements for salts containing ThF_4, UF_4, or both.

LiF-BeF_2-ThF_4: Cantor [75] cited a single specific heat of 0.324 cal/g*K at an unknown temperature. However, this value was based upon unpublished measurements by his co-author Dworkin and further details were not provided.

LiF-BeF_2-UF_4: No available specific heat data was found for this fuel salt.

LiF-BeF_2-ThF_4-UF_4: A single value at 700 °C was reported by Cohen et al [77] as 0.37 cal/g*K with 20% error. Cantor [75] listed values independent of temperature for four compositions which were estimated by mole fraction additivity with 4% error. Isochoric values were also calculated by Cantor for these compositions.

LiF-NaF-KF-ThF_4: Cohen et al [77] cited a 700 °C value with ± 20% error. The value is a calculation, rather than an experimental measurement.

LiF-NaF-KF-UF_4: Blalock and Powers [86] used an ice calorimeter to obtain a value of 0.44 cal/g*K over the temperature range 500-1000 °C. An appropriate uncertainty to this fuel mixture ("mixture 14") was listed at 6.8%. Powers [123] later presented results with ~1% error, which was large enough to mask an observed temperature dependence, and specific heat was assumed to be constant. However, Powers does not present a sample size or origin to his correlation equations. Finally, Cohen et al [77] presented two specific heats for two different compositions which were calculated rather than experimentally measured and assigned a ±20% error. Cohen's values reasonably resembled the above-mentioned results [86].

Table 11 Fuel salt specific heat capacity data reference.

Author	Year	Molar Composition (%)	Technique employed	c_p (cal/g*K)	Uncertainty quoted (%)	Temperature Range (K)	No. of Data	Form of Data
LiF - BeF_2 - ThF_4								
Cantor	1968	72 - 16 - 12	Cites unpublished measurements by Dworkin	0.324	-	-	1	A
LiF-BeF_2-UF_4								
N/A								
LiF - BeF_2 - ThF_4 - UF_4								
Cantor	*1968*	*73 - 16 - 10.7 - 0.3* *72 - 21 - 6.7 - 0.3* *68 - 20 - 11.7 - 0.3* *63 - 25 - 11.7 - 0.3*	*Calculation*	*See figure*	-	-	*3* *3* *3* *3*	*A*

Cantor	1968	73 - 16 - 10.7 - 0.3 72 - 21 - 6.7 - 0.3 68 - 20 - 11.7 - 0.3 63 - 25 - 11.7 - 0.3	Estimated by mole fraction additivity	0.34 0.39 0.33 0.33	4	-	1 1 1 1	A
Cohen et al.	1956	71 - 16 - 12 - 1	Estimate/ calculation	0.37	20	973	1	A
			LiF-NaF-KF-ThF_4					
Cohen et al.	1956	46.2 - 11.4 - 41.8 - 0.6	Estimate/ calculation	0.45	20	973	1	A
			LiF-NaF-KF-UF_4					
Blalock & Powers	1956	44.5 - 10.9 - 43.5 - 1.1	Ice calorimeter	0.44	6.8	773 - 1273	1	A
Cohen et al.	1956	44.7 - 11.0 - 40.3 - 4.0 45.3 - 11.2 - 41.0 - 2.5	Estimate/ calculation	0.38 0.41	20	973	1 1	A
Powers	1957	45.3 - 11.2 - 41.0 - 2.5	Experiment	0.399	1	-	1	A

**Italics* represent isochoric specific heats (c_v).

A = averages from data/equation, D = diagram, E = equation, T = tabulated experimental data

Thermal Conductivity

Figure 29 and Table 12 present thermal conductivity measurements for salts containing ThF_4, UF_4, or both.

LiF-BeF_2-ThF_4: No available thermal conductivity data was found for this fuel salt.

LiF-BeF_2-UF_4: No available thermal conductivity data was found for this fuel salt.

LiF-BeF2-ThF_4-UF_4: Cantor [75] submitted four thermal conductivity values for four molar compositions. Values were determined by a theoretical equation derived by Rao [124] and adapted to molten salts by Turnbull [125]. With an estimated error exceeding ±25%, this method will not be detailed further. Cooke [94] is the only source to have taken experimental values (Figure 29). In their work, heat shunting in the variable-gap apparatus for low conductivity salts was revised by applying a correction factor. This correction factor was based on gap spacing (which was derived from measurements with water, Hitec salt, and mercury), and then applied to MSRE fuel and coolant salts. However, complex coolant cell geometry led them to assume a uniform heat flux and wall temperature at 0 °C. No error was presented, but correction values for calibration liquids (water and Hitec salt) ranged from 5% to 15%, respectively. General error estimates for the variable gap technique are presented by Cooke in another paper [126].

LiF-NaF-KF-ThF_4: No available thermal conductivity data was found for this fuel salt.

LiF-NaF-KF-UF_4: "Mixture 14" by Cohen et al [77] was cited as 0.04 W/cm*°C from a paper by S.J. Claiborne (ORNL CF 553-1-233), which was not experimentally determined and assigned a 20% error by default.

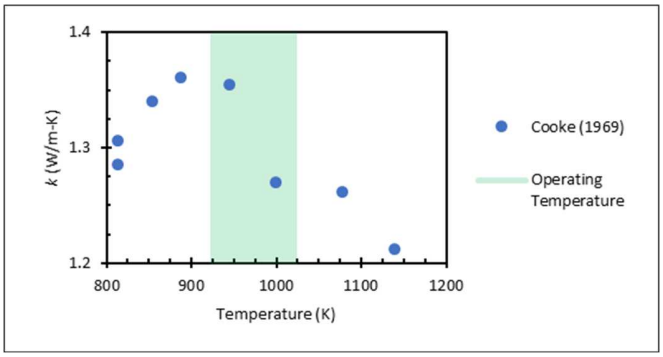

Figure 29 Thermal conductivity as a function of absolute temperature for LiF-BeF_2-ThF_4-UF_4. Strong deviation from expected trends necessitate more study into this composition.

Table 12 Fuel salt thermal conductivity data reference.

Author	Year	Molar Composition (%)	Technique employed	Uncertainty quoted (%)	Temperature Range (K)	No. of Data	Form of Data
LiF - BeF_2 - ThF_4							
N/A							
LiF-BeF_2-UF_4							
N/A							
LiF - BeF_2 - ThF_4 - UF_4							
Cantor	1968	73 - 16 - 10.7 - 0.3 72 - 21 - 6.7 - 0.3 68 - 20 - 11.7 - 0.3 63 - 25 - 11.7 - 0.3	Estimate given by theoretical equation adapted to molten salts	≥ 25	-	4	A
Cooke	1969	67.5 - 20 - 12 - 0.5	Absolute variable gap apparatus	-	813 - 1138	8	D
LiF-NaF-KF-ThF_4							
N/A							
LiF-NaF-KF-UF_4							
Cohen et al.	1956	44.5 - 10.9 - 43.5 - 1.1	(citing Claiborne S.J., ORNL CF 53-1-233.)	20	-	1	A

A = averages from data/equation, D = diagram, E = equation, T = tabulated experimental data

Electrical Conductivity

Figure 30 and Table 13 present electrical conductivity measurements for salts containing ThF_4, UF_4, or both.

LiF-BeF_2-ThF_4: Robbins and Gallanter [127] is the only known source for electrical conductivity measurements here. Eutectic information was unspecified and/or unknown; thus, all studied compositions are shown in Figure 30 and Table 13. All six tests fell short of an operating temperature of 700 °C. Clear trends can be seen, and it appears the conductivity varied directly with % LiF concentration. Uncertainty was calculated to be ± 3%. Robbins and Gallanter cited Robbins and Braunstein [101] for the measurement technique, which was a silica conductance cell. Because no

known reference standards existed for conductivity constants of molten salts, potassium nitrate was employed as a substitute for the concentration cell and measuring bridge devices.

LiF-BeF_2-UF_4: No available electrical conductivity data was found for this fuel salt.

LiF-BeF_2-ThF_4-UF_4: Cantor [75] cited empirically based relations for each composition studied based on analogous or related salts. The relationships were listed with 20% error.

LiF-NaF-KF-ThF_4: No available electrical conductivity data was found for this fuel salt.

LiF-NaF-KF-UF_4: No available electrical conductivity data was found for this fuel salt.

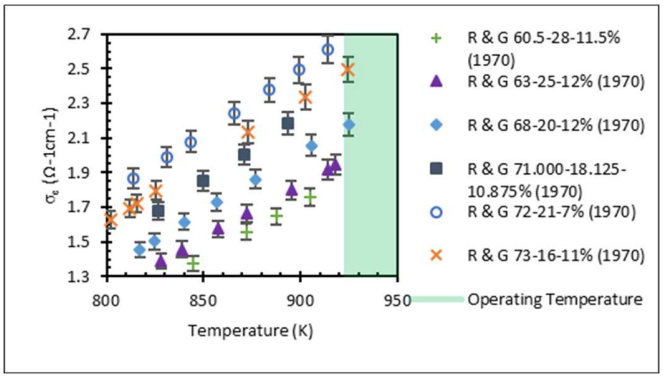

Figure 30 Electrical conductivity as a function of absolute temperature for LiF-BeF_2-ThF_4. All data are from a single study by Robbins and Gallanter (R & G) in 1970. X-X-X% indicates the percent molar composition of each respective element of LiF-BeF_2-ThF_4. An error of 3% was reported for all data.

Table 13 Fuel salt electrical conductivity data reference.

Author	Year	Molar Composition (%)	Technique employed	Uncertainty quoted (%)	Temperature Range (K)	No. of Data	Form of Data
LiF - BeF_2 - ThF_4							
Robbins & Gallanter	1970	73 - 16 - 11 72 -21 - 7 68 - 20 - 12 63 - 25 - 12 71.000 - 18.125 - 10.875 60.5 - 28 - 11.5	Silica concentration cell and measuring bridge	3	802 - 925 814 - 914 817 - 925 828 - 918 827 - 894 845 - 905	7 7 7 7 4 4	T
LiF-BeF_2-UF_4							
N/A							
LiF - BeF_2 - ThF_4 - UF_4							
Cantor	1968	73 - 16 - 10.7 - 0.3 72 - 21 - 6.7 0.3 68 - 20 - 11.7 - 0.3 63 - 25 - 11.7 - 0.3	Estimated empirical equations from data on analogous salts	20	-	-	E
LiF-NaF-KF-ThF_4							
N/A							
LiF-NaF-KF-UF_4							
N/A							

A = averages from data/equation, D = diagram, E = equation, T = tabulated experimental data

4. Methods of Analysis

Melting Point & Component Solubility

Phase diagrams are vital to understanding the overall performance of a molten salt through a wide range of conditions [128]. According to Williams et al [34], most all of the binary phase diagrams of interest have been investigated, though ternary diagrams are generally more lacking. Analytical modeling or estimation of phase diagrams may be unnecessary, but conflicts between models mentioned earlier in the report (i.e. van der Meer et al [118]) and experimental values necessitate a closer look into the systems where discrepancy is found. Furthermore, Beierschmitt [128] stated that the thermodynamic data necessary to construct these diagrams is currently pursued by too few research teams. Further, irradiation effects and compositional changes, especially at temperatures at and beyond MSR design temperatures, would necessitate the use of phase diagrams to further assess the impact of these factors on the salts.

For accurate melting temperature measurements, Molten Salt Workshop [23] recommended a simultaneous DSC and thermogravimetric analysis (DSC/TGA) to complement common XRD and electrical-based measurements. However, high standards of salt purity are required, and no national standard exists for salt purification, nor are large samples from commercial suppliers of sufficient purity for experimentation [23]. Moreover, historical phase diagrams often involved large sample sizes with unknown impurity contents; reconciliation between old and new diagrams is imperative [23].

Density

With exception, nearly all experimental values cited in this paper with regards to density were made using some application of Archimedes' Principle (Table 14). This is in part because experimental designs which utilize buoyancy measurements are relatively simple to set up and calibrate, even when working with high temperature melts. With an error of ± 1% for even the earliest designs, its reliability has made salt density one of the more well-known properties. Modifications allowing for error due to wetting and molten salts' relatively high surface tension would be an appropriate next step [129]–[131].

For more volatile mixtures, Cantor [119] devised a metal dilatometer which proved extremely accurate for nitrate and alkali fluoroborate salts, with a reproducibility of ±0.1%. He noted that modifications to the apparatus would result in even smaller error.

Clarno et al [7] reported that calculated densities based upon molar additivity allows for simple density predictions with about 5% error. Many calculated trend line references exist for the above listed compositions, particularly for salts including fissile elements. However, estimated values have not been included in either the relevant figures or Table 14 because primary experimental data was our focus. Sources with calculated values are specified as such in the reference tables above.

More recently, density prediction has been developed by use of the modified quasi-chemical model, relating the system's Gibbs energy to the molar volume [31].

Table 14 Density measurement methods.

Density			
Method	Advantages	Disadvantages	Error (%)

Archimedean Methods	Simple, easy to calibrate, reproducible results	Potential error due to wetting, not suitable for volatile liquids	<1
Calculation via Molar Additivity	Very quick estimate of density possible	Estimation not as accurate as experimental measurement	5
Dilatometer	High accuracy, metal dilatometers better for volatile liquids	More complex than the Archimedean method, must be recalibrated after multiple thermal cycles due to slight volumetric changes	~0.1

Viscosity

Viscosity of high temperature melts differs from ambient fluids in that the melt's experimental data can vary significantly from values predicted by the Arrhenius equation [132]. Viscosity measurements for molten salts are generally accomplished by one of five methods: efflux-cup (orifice), capillary, rotational, oscillating, and falling-body viscometry (Table 15).

As molten salts are Newtonian fluids [7], efflux cup and capillary viscometers are simple to operate, produce, and maintain while providing highly accurate results [74], [133]. Capillary viscometry is based upon the Hagen-Poiseuille equation for a fluid flowing through a capillary with a known pressure drop [132]. Greater precision is achieved with relative measurements, although absolute systems are possible [133]. Six assumptions govern the use of this method: a straight capillary with a known cross section, an incompressible fluid with constant density, a Newtonian fluid with pressure-caused viscosity variation deemed negligible, constant fluid temperature with negligible viscous dissipation, laminar and steady flow, and no fluid slip at the boundary wall. Any compromise of these assumptions must be accounted for with mathematical correction [132], [134]. It is important to note that efflux viscometers have produced irregular results with compositions containing beryllium [120] due to "humping" of the fluid surface during drainage [135]. Capillary viscometers must employ metal tubes as glass and quartz cannot handle the high temperature. Unfortunately, this makes laminar flow difficult to maintain (from metal's generally poorer surface finish) [132].

Rotational viscometers rely on the relationship between viscosity and torque applied by a fluid on a rotating surface. Their steady performance allows data to be taken continuously with the same sample while varying other parameters such as temperature [134]. Cohen and Jones described the behavior of a simple cylinder viscometer [74]. Rotational viscometers rely on previous calibration with a known fluid to obtain accurate results, but calibrations must be done with fluids of similar density and viscosity, especially as the cylinder-wall gap increases. Care must be taken to avoid turbulence or temperature rise from high rotation rates [134]. Error estimates can easily approach 10% [136].

Oscillatory-type viscometers observe the logarithmic decrement of amplitude and period decay of an oscillating, often torsional pendulum. The fluid provides friction to the object which can be calibrated against another known fluid viscosity. For highly corrosive substances at high temperature or pressure, an oscillating cup viscometer (where fluid rests on the inside of the oscillating body) is often used because of its small container volume [132]. A molten salt viscometer of this type by Tørklep and Øye matched water's viscosity values within 0.06% deviation and measured molten NaCl to within ±0.2% error [132]. While high temperatures are possible with the oscillating cup, the meniscus effect masks the exact height of fluid in the cup [132]. Tolbaru et al avoided this problem by running the sample at a full-cup condition [137].

Falling-ball viscometers utilize a sphere falling at constant velocity through the sample material in order to determine the sample's absolute viscosity, as modeled by Stokes' Law [132]. Besides requiring uniform ball and sample temperature, this method requires that the sphere move very slowly (Reynold's number less than unity) [132], [134], though corrections can be applied for Reynold's numbers as high as two [134]. Numerous corrections have been suggested for wall and end effects [132]–[134] as well. Though not as accurate as an oscillating cup viscometer, falling-

ball viscometers are more robust for handling molten salts while being simple and inexpensive to operate [138]. Measurement techniques traditionally employ optical methods, but X-ray and electromagnetic methods for opaque liquids are also effective [132]. An estimated error of ±0.2% has been obtained for standard operating conditions, though 1% is not atypical [132], [136].

Table 15 Viscosity measurement methods.

Viscosity			
Method	Advantages	Disadvantages	Error (%)
Orifice/ Capillary	Simple to produce and maintain, accurate, works for most liquids	Requires modification at high temperatures and corrections for violating its assumptions. Less accurate for beryllium melts.	0.3
Falling-Body	Simple, inexpensive, more robust than oscillating-body	Best for Re < 1, numerous corrections needed for wall effects	0.2 - 1
Oscillating-Body	Ideal for corrosive liquids in more extreme conditions, only small sample needed	Meniscus can mask exact liquid heights	0.2
Rotational-Body	Continuous data sampling due to steady operation	Must be calibrated with similar liquid sample, operating conditions must be well-controlled	10

Specific Heat (isobaric)

Most measurement techniques (Table 16) to measure specific heat historically involved drop calorimetry (specifically Bunsen-ice or copper block) or differential scanning calorimetry (DSC). Drop calorimetry involves 'dropping' a capsule of sample material into a controlled bath or furnace of known temperature and measuring the temperature change of the sample and bath. Total enthalpy change can be determined in the control, which then allows the calculation of the sample's specific heat capacity (often the 'slope' of the enthalpy data). The electrical characteristics of the substance may be neglected as no resistive heating is performed [100]. However, measuring times are long, and care must be taken so the corrosive salts do not react with the container walls when a container is used [100]. A well-calibrated drop calorimeter can attain 0.2-0.4% uncertainty [100], but designing an apparatus to this level of accuracy is both laborious and costly [100].

DSC's predecessor was differential thermal analysis, or DTA. DTA involved heating both a sample and reference material with a heater over a temperature range and noting the difference in final temperature between them. While a great step forward, this method was rarely considered fit for quantitative measurements due to the temperature difference being variable with other factors [100]. DSC is similar, but the desired temperature difference between both sample and reference is 0 °C. This involves heating both pans with two separate heaters over the temperature range. DSC often superimposes a sinusoidal temperature signal over a controlled temperature curve in order to directly measure the heat capacity of the salt [31]. DSC's temperature ramp rates (typically 10-50 K/min) are an order of magnitude higher than that of drop calorimetry, while the painstaking construction of equipment associated with drop calorimetry is not required for DSC procedures. DSC employs smaller sample sizes and while only relative specific heats are generated, these can be easily converted when using a well-documented reference material [100].

According to Clarno et al [7], old calorimeters were crude and estimated 10% error for their readings. A notable exception to this is FLiBe, which, due to the MSRE's relatively abundant data logging, has only ±2% error in its heat capacity [7]. However, with notable strides in controls and computer technology has come increased accuracy: ≤ 1% from 300 – 1000 K and ≤ 2% from 1000 – 2000 K [100]. For DSC specifically, error is approximately ± 1% for all

temperatures except from 800-1000 K, where error can creep up to 2.5% due to inconsistent radiative conditions when heating versus cooling [100].

The best theoretical estimate for heat capacity remains the Dulong and Petit method, which models heat capacity as temperature independent (based upon molar mass and atoms per molecule) within 20% error [7] [139].

Table 16 Specific heat capacity measurement methods.

Specific Heat Capacity (isobaric)			
Method	Advantages	Disadvantages	Error (%)
Differential Scanning Calorimetry (DSC)	Quicker measurements, less labor intensive than drop calorimetry, temperature kept constant	Only relative specific heats generated	1 - 2.5
Differential Thermal Analysis (DTA)	Quicker measurements, less labor intensive than drop calorimetry	Only relative specific heats generated	1 - 2.5
Drop Calorimetry	Electrical characteristics of salt can be neglected, based on simple theory	Long measuring times, high accuracy measurements are expensive, corrosive salts can damage container	0.2 - 10
Dulong-Petit Method	Simple, quick estimate of heat capacity	Assumes temperature independent liquid, high error	20

Thermal Conductivity

Thermal conductivity of molten salts remains the most difficult parameter to accurately measure. To measure this property, heat flow via only conduction (without convection or radiation) must be accurately known, in addition to the temperature distributions and fluxes. Often, unaccounted convective and radiative heat transfer leads to overestimations of thermal conductivity. Molten salts are nearly transparent to infrared radiation, and 10-35% error from radiation and natural convection can result when at high temperatures (500 K and higher) [6], [31]. McDonald noted that the salts' high electrical conductivity could render many transient measuring techniques using bare wire ineffectual [140], though insulated wire or liquid metal techniques have been pursued since then [141], [142]. Multiple techniques have been developed to reduce these errors for molten salts and will be discussed below (Table 17). These include: the parallel plate method, the concentric cylinders method, the transient hot-wire method, and the forced Rayleigh scattering method.

In the parallel plate method (PPM), the total heat transfer is measured between two horizontal plates over a temperature gradient. Convection and radiation must be minimized with both small plate separation and polished surfaces (lowering emissivity), respectively [132]. A guard can be installed to minimize lateral heat loss between the plates, though temperature difference between the hot plate and guard introduces another source of error[100]. At high temperatures, error is estimated to be between about 5-10% [100]. While applications have been found up to 1200 °C [100], PPM has been viewed as appropriate up to 500 °C, likely due to complexities in reducing radiative error with guards [132]. Assael et al concluded it was best for solids[6], with Cantor discouraging its use for poor thermally conductive fluids at elevated temperatures, such as molten salts [57]. Cantor recommended an improved apparatus which varied the gap between plates in order to reduce error [57], but detail on his method will not be given here.

The concentric cylinder method involves measurement of total heat between two isothermal, concentric cylinders separated by the sample fluid in order to calculate its thermal conductivity. Nearly the entire span of conductivity values in this paper employed the use of the concentric cylinders method, as it was widely regarded as an accurate measurement technique (1-3% error) [132]. Concentric cylinders can measure nearly any liquid regardless of electrical

conductivity or pressure [89]. However, a high degree of surface polishing and concentric alignment are necessary to reduce error, and cylinder surfaces with low emissivity are required to limit inaccuracies due to radiative heat transfer [132]. Assael et al [6] stated that few concentric cylinder measurements, if any, can be considered reliable because most authors did not take sufficient care to eliminate convection and radiation between the cylinder walls. As a result, error with temperature increase becomes grossly unacceptable due to the formation of a strong, positive temperature gradient. When Tufeu et al employed an extremely narrow gap to reduce natural convection and polished silver to reduce emissivity, error was still estimated at 4% [143]. Comments on the exact modifications by each author in relation to their method were given in previous sections, when available. Design considerations for constructing a radial heating apparatus are given by Maglić et al [100].

The transient hot-wire method uses a heating wire with constant, uniform heat flux radially heating a sample in thermal equilibrium. The slope of the temperature rising as a function of the natural logarithm of time is then used to determine the thermal conductivity of the sample. High conductivity samples shorten the linear region of the logarithmic time plot, and for this reason measurements were historically limited to materials with conductivities of 2.0 W/m*K unless alterations were made to the sample size and hot-wire [100], [144]. The advantage to this rapid transient method is that it curbs error due to natural convection. However, the measurement of non-transparent samples leads to a coupling of conduction and radiation, especially at high temperatures [132]. Luckily, if significant radiative error exists, it is manifest in additional curvature of the T-ln t curve [132]. The reliability over repeated measurements in harsh conditions was demonstrated by Daw et al [145]. Resistance values in the probes (and therefore power input) were generally constant with time, giving 6% error for low-conductance samples at high temperature. However, Daw noted sample container sizes must be chosen carefully to avoid edge effects, particularly based on the thermal diffusivity of the sample. For electrically conductive materials, such as molten salts, wire insulation is recommended to avoid current shunting, sample polarization, and distorted small-voltage signals [57], [132]. McDonald and Davis studied several molten alkali halides using a modified transient hot-wire technique [140] with quartz-insulation. However, Assael et al reported that this measurement technique was likely compromised because of unresolved convective error [6] manifesting as a positive temperature dependence. Assael's primary data set references works reporting about 3% error [141], [142], [146].

Forced Rayleigh scattering involves splitting a laser beam path and recombining them to create a diffraction pattern in the sample. This pattern creates a spatially sinusoidal temperature distribution whose decay is measured as a function of the imposed diffraction period. A second laser is passed through this pattern and its maximum phase variation and diffracted intensity enable the calculation of the sample's thermal diffusivity. It's short measurement time and small temperature change help to eliminate convective and radiative errors, and the technique is promising for high temperature molten salt measurements [132]. Forced Rayleigh scattering has been successfully employed in the thermal conductivity measurement of halide (iodide, bromide, and chloride) salts, but not to fluoride composed salts. Chloride salt conductivity measurements presented by Assael et al were listed with 4-11 % uncertainty, while bromide salts had less uncertainty (3-7%).

In the transient laser flash technique, the sample is placed below a thin metal disk or sandwiched between two metal disks. A laser pulse heats up the outside surface of the disk, and the temperature response is measured from either the back of the fluid or the outside of the bottom disc to derive the thermal conductivity. This method was used by Harada et al [147] for molten alkali halide salts but they reported 10% error. Assael et al [6] noted that Harada's was the only group utilizing this method to successfully obtain a negative temperature dependence, indicating that other researchers had not completely accounted for non-conductive heat losses.

Several significant theoretical predictions of the thermal conductivity of molten salt mixtures have been proposed. The first was proposed by Rao [124] and applied to molten salts by Turnbull [125]. Another model created from empirical data by Ignatiev et al is a function of temperature only [148]. Redkin et al reported that molar thermal conductivity was temperature independent for a salt, basing their model on this finding [149]. More recent models seek to implement

molecular dynamics simulations [89] or for binary mixtures based on their individual components [150] with a reported 6.4% error.

Table 17 Thermal conductivity measurement methods.

Thermal Conductivity			
Method	Advantages	Disadvantages	Error (%)
Concentric Cylinder	Pressure and conductivity independent, steady operation	Convection and radiation hard to minimize, high tolerances needed	1-4
Forced Rayleigh Scattering	Quick measurements minimize convective and radiative errors	Little if any measurements applied to fluoride salts	3-11
Parallel Plate Method (PPM)	Simple measurement technique	Error prone, suitable for low temperatures and solids	5-10
Transient Hot-Wire	Convective error inherently limited, radiative error manifested in log plot curvature	Generally limited to low thermal conductivities, wire insulation needed for electrically conductive samples	3-6
Transient Laser Flash	Transient technique should reduce error	Historic measurements do not generally account for non-conductive losses	10

Electrical Conductivity

Molten salts currently lack extensive electrical transport models, which necessitates experimental procedures for electrical conductivity data [127]. Molten salts are generally good electrical conductors and thus do not suffer from thermal emission of electrons or surface leakage as sources of error common for insulators [100]. Perhaps the most common source of inaccuracy in experimental measurements is the accumulation of error with higher environmental temperatures. Sample materials must be carefully selected in such cases, particularly from 1000-1200 K [100].

The most common form of conductivity measurement device is a silica conductance cell coupled with a Wheatstone bridge (Table 18). However, the parallel capacitor-resistor setup of the bridge is problematic because the resistance of the sample is in series with the capacitance [151]. Due to molten salts' high electrical conductivity (and therefore low measurement resistance), extremely high frequencies would be necessary to equate the two resistances. A bridge with a capacitor and resistor in series was constructed to reduce this error [151]. These low resistance cells also commonly employ platinum, as it is one of the few materials compatible with molten fluoride salts [115]. Electrodes pass current through the sample under a known voltage while measurements are taken of a sample geometry to obtain the cell constant. Analysis in the cell assumes uniformity of properties and composition, though exceptions to this rule may be made when deviations are averaged over a larger specimen size [100]. Thus, high sample purity is essential for accurate readings, particularly for fuel salts. Error measurements of ±0.3-3% are typically for molten salt measurements. Further discussion on the construction and calibration of conductivity cells is given by Robbins and Braunstein [112], [113], [152].

Table 18 Electrical conductivity measurement methods.

Electrical Conductivity			
Method	Advantages	Disadvantages	Error (%)

Conductance Cell with Bridge	Simple experimental setup, highly matured technique	Few cells durable for fluoride measurements, high purity required	0.3-3

Conclusion

In this review, we have presented the selection criteria for several candidate coolant and fuel salts for MSRs ($LiF\text{-}BeF_2$, $LiF\text{-}NaF\text{-}KF$, $KCl\text{-}MgCl_2$, $KF\text{-}ZrF_4$, and $NaF\text{-}KF\text{-}MgF_2$, with and without UF_4 and/or ThF_4). The density, viscosity, specific heat, melting point, thermal conductivity, and electrical conductivity based on original sources were presented to evaluate both salt suitability for MSRs and the need for further study. Particular attention was given to the uncertainty of the measurement method as a function of temperature, as well as an overview of the applicable measurement and their shortcomings.

To enable effective prediction and licensing of MSRs, new thermophysical property measurements with accurate techniques on fueled and non-fueled salts is necessary to fill the gaps in data identified in this review. Although density and viscosity possess the most prolific data, most methods lack uncertainty analyses for their data. However, the Archimedean method and oscillating cup viscometry have been well-proven in documenting these uncertainties, so the next step is to carefully evaluate more test specimens. The same argument could be made for heat capacity, with one difference. While several tests have been run for most of the candidate salts in this paper, most were done with drop calorimetry, which is often difficult to perform. With the widespread implementation of DSC, heat capacity measurements could be more rapidly performed over more salt compositions. Electrical conductivity possesses neither large data sets nor reliable precision but is important for resistive heating measurement techniques (i.e. hot-wire) and the intermolecular, ionic interactions of the salt. Finally, historical thermal conductivity measurements have large uncertainties, mostly due to inaccurate steady-state measurement techniques. Potential transient methods, such as transient hot-wire or Rayleigh scattering, were identified as potential methods for being the most promising in terms of accuracy and reliability.

Acknowledgements

This research is being performed using funding received from the DOE Office of Nuclear Energy's Nuclear Energy University Program, Award #DE-NE0008870. We thank David Pixton at the Harold B. Lee library for his significant help in obtaining many of these documents.

References

[1] R. B. Briggs, *Molten-salt Reactor Program Semiannual Progress Report: For the Period... For the Period Ending August 31, 1966*. Oak Ridge National Laboratory, 1967.

[2] P. Sabharwall, E. S. Kim, M. McKellar, N. Anderson, and M. Patterson, "Process heat exchanger options for the advanced high temperature reactor," INL/EXT-11-21584, June, 2011.

[3] C. W. Forsberg, P. F. Peterson, and P. S. Pickard, "Molten-salt-cooled advanced high-temperature reactor for production of hydrogen and electricity," *Nucl. Technol.*, vol. 144, no. 3, pp. 289–302, 2003.

[4] R. Yoshioka, "Nuclear Energy Based on Thorium Molten Salt," *Molten Salts Chem. Lab Appl.*, p. 471, 2013.

[5] R. R. Romatoski and L. W. Hu, "Fluoride salt coolant properties for nuclear reactor applications: A review," *Ann. Nucl. Energy*, vol. 109, pp. 635–647, Nov. 2017, doi: 10.1016/j.anucene.2017.05.036.

[6] M. J. Assael, K. D. Antoniadis, M. L. Huber, and W. A. Wakeham, "Reference Correlations for the Thermal Conductivity of 13 Inorganic Molten Salts," *J. Phys. Chem. Ref. Data*, vol. 47, no. 3, p. 033104, Sep. 2018, doi: 10.1063/1.5052343.

[7] K. Clarno *et al.*, *Trade Studies for the Liquid-Salt-Cooled Very High-Temperature Reactor: Fiscal Year 2006 Progress Report*. 2007.
[8] V. V. Kirichenko, "Molten Salt Applications for Nuclear Energy," VNIITF, Russia, Chelyabinsk reg., Snezhinsk, Project ISTC #3749, 2014.
[9] D. Holcomb, "Module 3: Overview of Fuel and Coolant Salt Chemistry and Thermal Hydraulics," Washington, D.C., Nov-2017.
[10] L. C. Olson, J. W. Ambrosek, K. Sridharan, M. H. Anderson, and T. R. Allen, "Materials corrosion in molten LiF–NaF–KF salt," *J. Fluor. Chem.*, vol. 130, no. 1, pp. 67–73, 2009.
[11] B. Kelleher, K. Dolan, P. Brooks, M. Anderson, and K. Sridharan, "Batch Scale Hydrofluorination of Li2BeF4 to Support Molten Salt Reactor Development," *J. Nucl. Eng. Radiat. Sci.*, vol. 1, Jun. 2015, doi: 10.1115/1.4030963.
[12] D. Petti *et al.*, "A Summary of the Department of Energy's Advanced Demonstration and Test Reactor Options Study," *Nucl. Technol.*, vol. 199, no. 2, pp. 111–128, Aug. 2017, doi: 10.1080/00295450.2017.1336029.
[13] A. Mourogov and P. Bokov, "Potentialities of the fast spectrum molten salt reactor concept: REBUS-3700," *Energy Convers. Manag.*, vol. 47, pp. 2761–2771, Oct. 2006, doi: 10.1016/j.enconman.2006.02.013.
[14] J. C. [ORNL] Gehin, D. E. [ORNL] Holcomb, G. F. [ORNL] Flanagan, B. W. [ORNL] Patton, R. L. [ORNL] Howard, and T. J. [ORNL] Harrison, "Fast Spectrum Molten Salt Reactor Options," United States, Jul. 2011.
[15] "Molten Salt Reactors," *World Nuclear Association*, Dec-2018. [Online]. Available: http://www.world-nuclear.org/information-library/current-and-future-generation/molten-salt-reactors.aspx.
[16] L. Luzzi, V. Di Marcello, and A. Cammi, *Multi-Physics Approach to the Modeling and Analysis of Molten Salt Reactors*. 2012.
[17] D. Krumwiede, R. Scarlat, J. K. Choi, T. M. Phan, and P. Peterson, "Three-dimensional modeling of the pebble-bed fluoride-salt-cooled, high-temperature reactor (PB-FHR) commercial plant design," *Trans. Am. Nucl. Soc.*, vol. 109, pp. 287–290, Nov. 2013.
[18] C. Forsberg, "Safety and Licensing Aspects of the Molten Salt Reactor," presented at the 2004 American Nuclear Society Annual Meeting, Pittsburgh, PA, Jun-2004.
[19] W. L. [Idaho N. L. Moe and A. [Southern C. Afzali, "Modernization of Technical Requirements for Licensing of Advanced Non-Light Water Reactors Selection and Evaluation of Licensing Basis Events," United States, Aug. 2019.
[20] R. O. Scarlat *et al.*, "Design and licensing strategies for the fluoride-salt-cooled, high-temperature reactor (FHR) technology," *Prog. Nucl. Energy*, vol. 77, pp. 406–420, 2014.
[21] N. R. Brown, D. J. Diamond, S. Bajorek, and R. Denning, "Thermal-Hydraulic and Neutronic Phenomena Important in Modeling and Simulation of Liquid-Fuel Molten Salt Reactors," *Nucl. Technol.*, vol. 206, no. 2, pp. 322–338, Feb. 2020, doi: 10.1080/00295450.2019.1590077.
[22] B. R. [Oak R. N. Lab. (ORNL) Betzler Oak Ridge, TN (United States)] (ORCID:0000000184259711), F. [Argonne N. Lab. (ANL) Heidet Argonne, IL (United States)], B. [Argonne N. Lab. (ANL) Feng Argonne, IL (United States)], C. [Idaho N. Lab. (INL) Rabiti Idaho Falls, ID (United States)] (ORCID:0000000184259711), T. [Argonne N. Lab. (ANL) Sofu Argonne, IL (United States)], and N. R. [Univ. of T. Brown Knoxville, TN (United States)], "Modeling and simulation functional needs for molten salt reactor licensing," *Nucl. Eng. Des.*, Aug. 2019, doi: 10.1016/j.nucengdes.2019.110308.
[23] "Molten Salt Chemistry Workshop," Oak Ridge National Laboratory, Apr. 2017.
[24] D. F. Williams and K. T. Clarno, "Evaluation of Salt Coolants for Reactor Applications," *Nucl. Technol.*, vol. 163, no. 3, pp. 330–343, 2008, doi: 10.13182/NT08-A3992.
[25] D. Holcomb and S. Cetiner, *An Overview of Liquid-Fluoride-Salt Heat Transport Systems*. 2010.
[26] W. R. Grimes, D. R. Cuneo, F. F. Blankenship, G. W. Keilholtz, H. F. Poppendick, and M. T. Robinson, "Chemical Aspects of Molten Fluoride Salt Reactor Fuels," in *Fluid Fueled Reactors*, J. A. Lane et al., Ed. Addison-Wesley NY, 1958.
[27] M. S. Sohal, M. A. Ebner, P. Sabharwall, and P. Sharpe, "Engineering Database of Liquid Salt Thermophysical and Thermochemical Properties," United States, Mar. 2010.
[28] L. V. Jones *et al.*, "Phase Equilibria in the Ternary Fused-Salt System LiF-BeF2,-UF4," *J. Am. Ceram. Soc.*, vol. 45, no. 2, pp. 79–83, 1962, doi: 10.1111/j.1151-2916.1962.tb11084.x.

[29] C. N. A. C. Z. Bahri, W. M. Al-Areqi, M. 'Izzat F. M. Ruf, and A. Ab. Majid, "Characteristic of molten fluoride salt system LiF-BeF2 (Flibe) and LiF-NaF-KF (Flinak) as coolant and fuel carrier in molten salt reactor (MSR)," *AIP Conf. Proc.*, vol. 1799, no. 1, p. 040008, Jan. 2017, doi: 10.1063/1.4972932.
[30] Rabald, "Reactor handbook second edition in four volumes vol. 1: Materials. published under contract with the U. S. Atomic energy commission, volume 1 edited by C. R. Tipton, jr., New York 1960, Interscience Publishers, Inc. New York 1, N. Y.; Interscience Publishers Ltd., London, Preis $ 36,50," *Mater. Corros.*, vol. 12, no. 2, pp. 126–126, Feb. 1961, doi: 10.1002/maco.19610120218.
[31] J. Ambrosek, *Molten Chloride Salts for Heat Transfer in Nuclear Systems*. 2011.
[32] D. F. Williams, "Assessment of Candidate Molten Salt Coolants for the NGNP/NHI Heat-Transfer Loop," *Oak Ridge Natl. Lab.*, no. ORNL0TM-2006069, 2006.
[33] R. Serrano-López, J. Fradera, and F. Cuesta-López, "Molten salts database for energy applications," 2013.
[34] D. F. Williams, L. M. Toth, and K. T. Clarno, "Assessment of Candidate Molten Salt Coolants for the Advanced High-Temperature Reactor (AHTR)," *Oak Ridge Natl. Lab.*, no. ORNL/TM-2006/12, 2006.
[35] T. B. Douglas and J. L. Dever, "Lithium Fluoride: Heat Content from 0 to 900°, the Melting Point and Heat of Fusion1," *J. Am. Chem. Soc.*, vol. 76, no. 19, pp. 4826–4829, Oct. 1954, doi: 10.1021/ja01648a016.
[36] R. E. Thoma, G. M. Hebert, H. Insley, and H. A. Friedman, "Equilibrium phase diagram of the lithium fluoride-beryllium fluoridezirconium fluoride system," *J. Nucl. Mater.*, vol. 27, no. 2, pp. 166–180, Jan. 1968, doi: 10.1016/0022-3115(68)90120-7.
[37] G. J. Janz, C. B. Allen, N. P. Bansal, R. M. Murphy, and R. P. T. Tomkins, *Physical Properties Data Compilations Relevant to Energy Storage. II. Molten Salts: Data on Single and Multi-Component Systems*, vol. 61. National Bureau of Standards, 1979.
[38] D. R. Lide, Ed., *CRC Handbook of Chemistry and Physics*, vol. 128. Boca Raton, FL: CRC Press, 2005.
[39] K. A. Romberger, J. Braustein, and R. E. Thoma, "New electrochemical measurements of the liquidus in the lithium fluoride-beryllium fluoride system. Congruency of lithium beryllium fluoride (Li2BeF4)," *J. Phys. Chem.*, vol. 76, no. 8, pp. 1154–1159, Apr. 1972, doi: 10.1021/j100652a012.
[40] A. G. Bergman and E. P. Dergunov, *Comptes Rendus Académie Sci. URSS*, p. 31,754, 1941.
[41] D. J. Rogers, T. Yoko, and G. J. Janz, "Fusion properties and heat capacities of the eutectic lithium fluoride-sodium fluoride-potassium fluoride melt," *J. Chem. Eng. Data*, vol. 27, no. 3, pp. 366–367, Jul. 1982, doi: 10.1021/je00029a041.
[42] G. J. Janz and R. P. T. Tomkins, *Physical properties data compilations relevant to energy storage. IV. molten salts: data on additional single and multi-component salt systems*, vol. nsrds-nbs61p4. National Bureau of Standards, 1981.
[43] "FactSage FTsalt salt database List of systems and phases." .
[44] W. D. Robertson, "BINARY PHASE DIAGRAMS OF HALIDE SALTS," YALE-2723; Vol.2 United States NTIS DTIE English, 1966.
[45] H. J. Seifert and H. Fink, *Thermal Analysis: 4th ICTA : [proceedings of the Fourth International Conference on Thermal Analysis Held at Budapest, Hungary, July 8-13, 1974]. Organic and macromolecular chemistry, earth sciences. Vol. 2*, vol. 2. Heyden, 1975.
[46] R. E. Thoma and W. R. Grimes, "Phase Equilibrium Diagrams For Fused Salt Systems," *Oak Ridge Natl. Lab.*, no. W-7485-eng-26, 1957.
[47] E. A. Alekszeeva and V. I. Poszipajko, *Diagrams of Melting for Salt Systems (Diagrammi plavkoszti solevih sisztem)*. Moscow: Metallurgy Publ. Co., 1977.
[48] R. E. Thoma, "Phase Diagrams of Nuclear Reactor Materials," *Oak Ridge Natl. Lab.*, no. ORNL-2548, 1959.
[49] A. G. Bergman and E. P. Dergunov, *Comptes Rendus Académie Sci. URSS*, vol. 48, no. 330, 1945.
[50] F. M. Jaeger and J. Khan, "XV. The Determination of the Specific Gravity of molten Salts and of the Temperature-Coefficient of their Molecular surface-energy," in *Investigations on the Temperature-Coefficients of the Free Molecular Surface-Energy of Liquids between -80 and 1650C.*, vol. 19, Amsterdam: KNAW, Proceedings, 1917, pp. 381–397.
[51] I. S. Yaffe and E. R. van Artsdalen, "Chemistry Division semiannual progress report: for period ending June 20, 1956," Oak Ridge National Laboratory, Oak Ridge, Tenn, ORNL-2159, 1956.
[52] B. C. Blanke, E. N. Bousquet, M. L. Curtis, and E. L. Murphy, "DENSITY AND VISCOSITY OF FUSED MIXTURES OF LITHIUM, BERYLLIUM, AND URANIUM FLUORIDES," MLM-1086 United States NTIS DTIE English, 1956.

[53] B. C. Blanke, E. N. Bousquet, L. V. Jones, E. L. Murphy, and R. E. Vallee, “DENSITY OF FUSED MIXTURES OF SODIUM FLUORIDE, BERYLLIUM FLUORIDE, AND URANIUM FLUORIDE,” MLM-1076 United States 10.2172/4331902 NTIS DTIE English, 1956.
[54] G. W. Mellors and S. Senderoff, “The Density and Surface Tension of Molten Fluorides,” *J. Electrochem. Soc.*, vol. 111, no. 12, 1964, doi: 10.1149/1.2426003.
[55] D. G. Hill, S. Cantor, and W. T. Ward, “Molar volumes in the LiF-ThF4 system,” *J. Inorg. Nucl. Chem.*, vol. 29, no. 1, pp. 241–243, Jan. 1967, doi: 10.1016/0022-1902(67)80163-5.
[56] B. Porter and R. E. Meaker, *Density and molar volumes of binary fluoride mixtures /*. Washington, D.C.: U.S. Dept. of the Interior, Bureau of Mines, 1966.
[57] S. Cantor, “Density and viscosity of several molten fluoride mixtures,” ORNL-TM-4308 United States 10.2172/4419855 Dep. NTIS ORNL English, 1973.
[58] G. J. Janz, G. L. Gardner, U. Krebs, and R. P. T. Tomkins, “Molten Salts: Volume 4, Part 1, Fluorides and Mixtures Electrical Conductance, Density, Viscosity, and Surface Tension Data,” *J. Phys. Chem. Ref. Data*, vol. 3, no. 1, pp. 1–115, 1974, doi: 10.1063/1.3253134.
[59] S. Cantor, W. T. Ward, and C. T. Moynihan, “Viscosity and Density in Molten BeF2–LiF Solutions,” *J. Chem. Phys.*, vol. 50, no. 7, pp. 2874–2879, 1969, doi: 10.1063/1.1671478.
[60] S. I. Cohen and T. N. Jones, “A SUMMARY OF DENSITY MEASUREMENTS ON MOLTEN FLUORIDE MIXTURES AND A CORRELATION FOR PREDICTING DENSITIES OF FLUORIDE MIXTURES,” *Oak Ridge Natl. Lab.*, Jul. 1954.
[61] J. Cibulková, M. Chrenková, R. Vasiljev, V. Kremenetsky, and M. Boča, “Density and Viscosity of the (LiF + NaF + KF)eut (1) + K2TaF7 (2) + Ta2O5 (3) Melts,” *J. Chem. Eng. Data*, vol. 51, no. 3, pp. 984–987, May 2006, doi: 10.1021/je050490g.
[62] J.-H. Cheng *et al.*, “A Device for Measuring the Density and Liquidus Temperature of Molten Fluorides for Heat Transfer and Storage,” *Chin. Phys. Lett.*, vol. 30, no. 12, 2013, doi: 10.1088/0256-307x/30/12/126501.
[63] G. J. Janz *et al.*, “Molten salts: Volume 4, part 2, chlorides and mixtures—electrical conductance, density, viscosity, and surface tension data,” *J. Phys. Chem. Ref. Data*, vol. 4, no. 4, pp. 871–1178, 1975, doi: 10.1063/1.555527.
[64] K. Grjotheim, J. L. Holm, B. Lillebuen, and H. A. Øye, “Densities and excess molar volumes of binary and ternary melts of MgCl2, CaCl2 and AlkCl,” *Trans. Faraday Soc.*, vol. 67, no. 0, pp. 640–648, 1971, doi: 10.1039/TF9716700640.
[65] J. N. Reding, “Densities and Molar Volumes of Molten Magnesium Chloride, Potassium Chloride, and Barium Chloride Mixtures,” *J. Chem. Eng. Data*, vol. 10, no. 1, pp. 1–4, Jan. 1965, doi: 10.1021/je60024a001.
[66] R. W. Huber, E. V. Potter, and H. W. S. Clair, *Electrical conductivity and density of fused binary mixtures of magnesium chloride and other chlorides*. U.S. Dept. of the Interior, Bureau of Mines, 1952.
[67] L. Yuanyuan, X. Xiankun, X. Wang, P. Li, Q. Hao, and B. Xiao, “Survey and evaluation of equations for thermophysical properties of binary/ternary eutectic salts from NaCl, KCl, MgCl2, CaCl2, ZnCl2 for heat transfer and thermal storage fluids in CSP,” *Sol. Energy*, vol. 152, pp. 57–79, Aug. 2017, doi: 10.1016/j.solener.2017.03.019.
[68] S. R. Darienko, Y. F. Chervinskii, V. N. Desyatnik, and S. F. Katyshev, “Density and Surface Tension of Melts of the KF-KCL-ZrF4 System,” *At. Energiya*, vol. 65, pp. 223–224, 1988.
[69] M. M. Vetyukov and G. I. Sipriya, “Viscosity of Melts in the Systems LiF-AlF3 and Na3AlF6-Li3AlF6,” *J. Appl. Chem. USSR*, vol. 36, no. 9, pp. 1849–1852, 1963.
[70] V. N. Desyatnik, A. I. Nechaev, and Y. F. Chervinskii, “Viscosity of Uranium Tetrafluoride-Lithium Fluoride Melts,” *Russ. J. Phys. Chem.*, vol. 53, no. 4, pp. 555–556, 1979.
[71] V. N. Desyatnik, A. I. Nechaev, and Y. F. Chervinskii, “Viscosity of Molten Mixtures of Beryllium Fluoride with Lithium and Sodium Fluorides,” *J. Appl. Chem. USSR USA*, vol. 54, no. 10, pp. 2035–2037, 1981.
[72] T. Ejima, Y. Sato, S. Yaegashi, T. Kijima, E. Takeuchi, and K. Tamai, “Viscosity of Molten Alkali Fluorides,” *J. Jpn. Inst. Met.*, vol. 51, no. 4, pp. 328–337, 1987.
[73] Y. Abe, O. Kosugiyama, and A. Nagashima, “Viscosity of LiF-BeF2 eutectic mixture (XBeF2 = 0.328) and LiF single salt at elevated temperatures,” *J. Nucl. Mater.*, vol. 99, no. 2, pp. 173–183, Sep. 1981, doi: 10.1016/0022-3115(81)90186-0.
[74] S. I. Cohen and T. N. Jones, “Viscosity Measurements on Molten Fluoride Mixtures,” *Oak Ridge Natl. Lab.*, Jun. 1957.

[75] S. Cantor, “PHYSICAL PROPERTIES OF MOLTEN-SALT REACTOR FUEL, COOLANT, AND FLUSH SALTS,” ORNL-TM-2316 United States 10.2172/4492893 Dep. CFSTI. ORNL English, 1968.
[76] S. I. Cohen and T. N. Jones, “MEASUREMENT OF THE VISCOSITY OF COMPOSITIONS 12, 14, AND 107,” United States, May 1956.
[77] S. I. Cohen, W. D. Powers, and N. D. Greene, “A PHYSICAL PROPERTY SUMMARY FOR FLUORIDE MIXTURES,” ORNL-2150(Del.) United States NTIS ORNL English, 1956.
[78] A. Merzlyakov, V. Ignatiev, and S. Abalin, “Viscosity of LiF–NaF–KF eutectic and effect of cerium trifluoride and uranium tetrafluoride additions,” *Nucl. Eng. Des.*, vol. 278, pp. 268–273, Oct. 2014, doi: 10.1016/j.nucengdes.2014.07.037.
[79] B. Vriesema, *Aspects of molten fluorides as heat transfer agents for power generation*. 1979.
[80] X. An, J.-H. Cheng, T. su, and P. Zhang, *Determination of thermal physical properties of alkali fluoride/carbonate eutectic molten salt*, vol. 1850. 2017.
[81] S. R. Darienko, S. P. Raspopin, and Y. F. Chervinskii, “Viscosity of Melts of the Reciprocal Ternary System K, Zr//F, Cl,” *At. Energiya*, vol. 62, pp. 122–124, 1987.
[82] A. C. Macleod, “High-temperature thermodynamic properties of the alkali-metal fluorides,” *J. Chem. Soc. Faraday Trans. 1 Phys. Chem. Condens. Phases*, vol. 69, no. 0, pp. 2026–2035, 1973, doi: 10.1039/F19736902026.
[83] M. W. Chase, “NIST-JANAF Thermochemical Tables, 4th ed.,” *J. Phys. Chem. Ref. Data Monogr. 9*, 1998, doi: 10.18434/T42S31.
[84] M. W. Rosenthal, R. B. Briggs, and P. R. Kasten, “Molten-salt Reactor Program Semiannual Progress Report for Period Ending August 31, 1968,” *Oak Ridge Natl. Lab.*, no. ORNL-4344, 1968.
[85] T. B. Douglas and W. H. Payne, “Measured Solid Enthalpy and Derived Thermodynamic Properties of and Liquid Lithium Tetrafluoroberyllate, from 273 to 900 K,” *Inst. Basic Stand. Natl. Bur. Stand.*, vol. 73A, no. 5, pp. 479–485, May 1969.
[86] W. D. Powers and G. C. Blalock, “ENTHALPIES AND HEAT CAPACITIES OF SOLID AND MOLTEN FLUORIDE MIXTURES,” ORNL-1956(Del.) United States NTIS ORNL English, 1956.
[87] V. Khokhlov, I. Korzun, V. Dokutovich, and E. Filatov, “Heat capacity and thermal conductivity of molten ternary lithium, sodium, potassium, and zirconium fluorides mixtures,” *J. Nucl. Mater.*, vol. 410, no. 1, pp. 32–38, Mar. 2011, doi: 10.1016/j.jnucmat.2010.12.306.
[88] A. E. Gheribi and P. Chartrand, “Thermal conductivity of molten salt mixtures: Theoretical model supported by equilibrium molecular dynamics simulations,” *J. Chem. Phys.*, vol. 144, no. 8, p. 084506, Feb. 2016, doi: 10.1063/1.4942197.
[89] A. E. Gheribi, J. A. Torres, and P. Chartrand, *Recommended values for the thermal conductivity of molten salts between the melting and boiling points*, vol. 126. 2014.
[90] K. Sreenivasan and M. Altman, “The Determination of Thermal Diffusivities of Thermal Energy Storage Materials: Part II—Molten Salts Beyond the Melting Point,” *J. Eng. Power*, vol. 91, no. 3, pp. 189–197, Jul. 1969, doi: 10.1115/1.3574731.
[91] M. V. Smirnov, V. A. Khokhlov, and E. S. Filatov, “Thermal conductivity of molten alkali halides and their mixtures,” *Electrochimica Acta*, vol. 32, no. 7, pp. 1019–1026, 1987, doi: 10.1016/0013-4686(87)90027-2.
[92] D. A. P. Jaworske and W. D. Perry, “Hot filament technique for measuring the thermal conductivity of molten lithium fluoride,” presented at the AIChE Summer National Meeting Session on Space Power Systems Technology, San Diego, CA, United States, 1990.
[93] E. F. M. Van der Held, J. Hardebol, and J. Kalshoven, “On the measurement of the thermal conductivity of liouids by a non-stationary method,” *Physica*, vol. 19, no. 1–12, pp. 203–216, 1953, doi: 10.1016/S0031-8914(53)80022-4.
[94] J. W. Cooke, “Thermophysical Properties,” Oak Ridge National LAboratory, Progress Report ORNL-4449, Feb. 1970.
[95] L. Cooper and S. J. Claiborne, “MEASUREMENT OF THE THERMAL CONDUCTIVITY OF FLINAK,” Aug. 1952, doi: 10.2172/4348011.
[96] C. T. Ewing, J. R. Spann, and R. R. Miller, “Radiant Transfer of Heat in Molten Inorganic Compounds at High Temperatures,” *J. Chem. Eng. Data*, vol. 7, no. 2, pp. 246–250, Apr. 1962, doi: 10.1021/je60013a028.
[97] Y. Ueki, N. Fujita, J. Yagi, M. Shibaraha, and A. Sagara, “Thermal conductivity measurement of fluoride molten salt FLiNaK by transient hot-wire method,” *High Temp. - High Press.*, vol. 46, no. 3, pp. 247–254, Jan. 2017.

[98] X.-H. An, J.-H. Cheng, H.-Q. Yin, L.-D. Xie, and P. Zhang, “Thermal conductivity of high temperature fluoride molten salt determined by laser flash technique,” *Int. J. Heat Mass Transf.*, vol. 90, pp. 872–877, Nov. 2015, doi: 10.1016/j.ijheatmasstransfer.2015.07.042.
[99] P. Polyakov and E. Gildebrandt, *Investigation of the thermal conductivity of melts of the system KCl-MgCl2*, vol. 12. 1974.
[100] K. D. Maglić, A. Cezairliyan, and V. E. Peletsky, *Compendium of thermophysical property measurement methods: Vol. 1, survey of measurement techniques*, vol. 1. Plenum Press, 1984.
[101] G. D. Robbins and J. Braunstein, “Specific Conductance of Molten Potassium Nitrate,” *J. Electrochem. Soc.*, vol. 116, no. 9, pp. 1218–1221, Sep. 1969, doi: 10.1149/1.2412282.
[102] V. Daněk, “Chapter 8 - Electrical Conductivity,” in *Physico-Chemical Analysis of Molten Electrolytes*, V. Daněk, Ed. Amsterdam: Elsevier Science, 2006, pp. 327–357.
[103] R. A. Perkins, H. M. Roder, and C. A. Nieto de Castro, “A High-Temperature Transient Hot-Wire Thermal Conductivity Apparatus for Fluids.,” *J. Res. Natl. Inst. Stand. Technol.*, vol. 96, no. 3, pp. 247–269, Jun. 1991, doi: 10.6028/jres.096.014.
[104] E. W. Yim and M. Feinleib, “Electrical Conductivity of Molten Fluorides II . Conductance of Alkali Fluorides, Cryolites, and Cryolite-Base Melts,” *J. Electrochem. Soc.*, vol. 104, no. 10, pp. 626–630, Oct. 1957, doi: 10.1149/1.2428430.
[105] E. W. Yim and M. Feinleib, “Electrical Conductivity of Molten Fluorides I . Apparatus and Method,” *J. Electrochem. Soc.*, vol. 104, no. 10, pp. 622–626, Oct. 1957, doi: 10.1149/1.2428429.
[106] H. Winterhager and L. Werner, *Bestimmung des elektrischen Leitvermögens geschmolzener Fluoride*, vol. 438. Springer-Verlag, 1957.
[107] E. A. Brown and B. Porter, *Electrical conductivity and density of molten systems of uranium tetrafluoride and thorium fluoride and alkali fluorides*. Washington, D.C.: U.S. Dept. of the Interior, Bureau of Mines, 1964.
[108] K. Matiasovsky, M. Malinovsky, and V. Danek, “Specific Electrical Conductivity of Molten Fluorides,” *Electrochimica Acta*, vol. 15, pp. 25–32, 1970.
[109] K. Matiasovsky, V. Danek, and B. Lillebuen, “On the Frequency and Temperature-Dependence of the Conductivity of Molten Salts,” *Electrochimica Acta*, vol. 17, pp. 463–469, 1972.
[110] V. Danek, M. Malinovsky, and K. Matiasovsky, “Elektrická vodivosť tavenín v sústavách LiF—AlF3 a LiF—Na3AlF6,” *Chem. Zvesti*, vol. 22, pp. 641–647, 1968.
[111] E. A. Balakir, Yu. G. Bushuev, and Yu. V. Kudryavtsev, “Investigation of the Electric Conductivity of Melts of Alkali Fluorides and Chlorides Depending Upon the Temperature,” *Sib. Chem. J.*, vol. 2, pp. 164–166, Apr. 1968.
[112] G. D. Robbins and J. Braunstein, “MEASUREMENT OF SPECIFIC CONDUCTANCE IN LiF-BeF2, (66-34 MOLE X),” *Oak Ridge Natl. Lab.*, no. ORNL-4254, pp. 144–146, 1968.
[113] G. D. Robbins and J. Braunstein, “IMPROVED DETERMINATION OF ELECTRICAL CONDUCTANCE OF LiF-BeF2 (66-34 MOLE %),” *Oak Ridge Natl. Lab.*, no. ORNL-4449, pp. 141–142, 1969.
[114] G. D. Robbins and J. Braunstein, “ELECTRICAL CONDUCTIVITIES AND IONIC MOBILITIES IN THE MOLTEN LiF-BeF2 SYSTEM,” *Oak Ridge Natl. Lab.*, no. ORNL 4548, 1970.
[115] N. D. Greene, “MEASUREMENTS OF THE ELECTRICAL CONDUCTIVITY OF MOLTEN FLUORIDES,” CF-54-8-64 United States 10.2172/4282414 ORNL English, 1954.
[116] R. E. Thoma, H. Insley, H. A. Friedman, and C. F. Weaver, “PHASE EQUILIBRIA IN THE SYSTEMS BeF2-ThF4 AND LiF-BeF2-ThF4,” *J. Phys. Chem.*, vol. 64, no. 7, pp. 865–870, Jul. 1960, doi: 10.1021/j100836a010.
[117] E. Capelli, “THERMODYNAMIC CHARACTERIZATION OF SALT COMPONENTS FOR MOLTEN SALT REACTOR FUEL,” 2016.
[118] J. P. M. van der Meer, R. J. M. Konings, and H. A. J. Oonk, “Thermodynamic assessment of the LiF–BeF2–ThF4–UF4 system,” *J. Nucl. Mater.*, vol. 357, no. 1, pp. 48–57, Oct. 2006, doi: 10.1016/j.jnucmat.2006.05.042.
[119] S. Cantor, “Metal Dilatometer for Determining Density and Expansivity of Volatile Liquids at Elevated Temperature,” *Rev. Sci. Instrum.*, vol. 40, no. 7, pp. 967–968, Jul. 1969, doi: 10.1063/1.1684132.
[120] H. G. MacPherson, “MOLTEN-SALT REACTOR PROJECT QUARTERLY PROGRESS REPORT,” *Oak Ridge Natl. Lab.*, no. ORNL-2684, Jan. 1959.
[121] H. G. MacPherson, “MOLTEN-SALT REACTOR PROJECT QUARTERLY PROGRESS REPORT,” *Oak Ridge Natl. Lab.*, no. ORNL-2723, pp. 38–43, Apr. 1959.

[122] H. G. MacPherson, “MOLTEN-SALT REACTOR PROGRAM QUARTERLY PROGRESS REPORT,” *Oak Ridge Natl. Lab.*, no. ORNL-2890, 1959.
[123] W. D. Powers, “Physical Properties,” *Aircr. Nucl. Propuls. Proj. Q. Prog. Rep.*, pp. 103–105, Jun. 1957.
[124] M. R. Rao, “Thermal Conductivity of Liquids,” *Phys. Rev.*, vol. 59, no. 2, pp. 212–212, Jan. 1941, doi: 10.1103/PhysRev.59.212.
[125] A. G. Turnbull, “THE THERMAL CONDUCTIVITY OF MOLTEN SALTS. II. THEORY AND RESULTS FOR PURE SALTS,” *Aust. J Appl Sci*, Sep. 1961.
[126] J. W. Cooke, “Development of the variable-gap technique for measuring the thermal conductivity of fluoride salt mixtures,” ; OAK RIDGE NATIONAL LAB., TENN., ORNL-4831 United States 10.2172/4556565 Dep. NTIS ORNL English, 1973.
[127] G. D. Robbins and A. S. Gallanter, “ELECTRICAL CONDUCTIVITIES OF PROPOSED MSBR FUEL COMPOSITIONS IN THE LiF-BeF2-ThF4 SYSTEM,” *MOLTENSALT React. PROGRAM Semiannu. Prog. Rep.*, pp. 159–161, Feb. 1970.
[128] K. Beierschmitt, “Basic Research Needs Workshop for Future Nuclear Energy, Report of the Basic Energy Sciences Workshop for Future Nuclear Energy,” Department of Energy, 2017.
[129] J. McCuan, “Archimedes Revisited,” *Milan J. Math.*, vol. 77, no. 1, p. 385, Sep. 2009, doi: 10.1007/s00032-009-0099-2.
[130] T. Fujisawa, T. Utigard, and J. M. Toguri, “Surface tension and density of the molten PbCl2–KCl–NaCl ternary system,” *Can. J. Chem.*, vol. 63, no. 5, pp. 1132–1138, May 1985, doi: 10.1139/v85-192.
[131] K. Yajima, H. Moriyama, Y. Tominaga, T. Hara, and J. Oishi, “Surface tensions of lithium fluoride-thorium fluoride binary melts and lithium fluoride-beryllium fluoride-thorium fluoride ternary melts,” *J. Chem. Eng. Data*, vol. 29, no. 2, pp. 122–124, Apr. 1984, doi: 10.1021/je00036a005.
[132] W. A. Wakeham, A. Nagashima, J. V. Sengers, International Union of Pure and Applied Chemistry., and Commission on Thermodynamics., *Measurement of the transport properties of fluids*. Oxford [England]; Boston; Boca Raton, Fla.: Blackwell Scientific Publications ; Distributed in the USA and North America by CRC Press, 1991.
[133] A. Dinsdale and F. Moore, *Viscosity and its measurement*. Published on behalf of the Institute of Physics and the Physical Society by Chapman and Hall, 1962.
[134] J. R. Van Wazer, J. W. Lyons, K. Y. Kim, and R. E. Colwell, *Viscosity and Flow Measurement; A Laboratory Handbook of Rheology, by J.R. Van Wazer (And Others)*. New York: Interscience Publishers, 1966.
[135] W. D. Powers, “Physical Property Measurements,” *MOLTEN-SALT React. PROGRAM Q. Prog. Rep. PERIOD End. JUNE 30 1958*, pp. 38–39, Jun. 1958.
[136] A. S. Morris and R. Langari, “Chapter 21 - Summary of Other Measurements,” in *Measurement and Instrumentation: Theory and Application*, 2nd ed., Academic Press, 2016, pp. 633–672.
[137] D. Tolbaru, R. Borcan, and S. Zuca, “Viscosity Measurements on Molten Salts with an Oscillating Cup Viscometer: Viscosity of Molten KNO3 and NaCl,” *Berichte Bunsenges. Für Phys. Chem.*, vol. 102, no. 10, pp. 1387–1392, 1998.
[138] M. Groesbeck and N. Balaich, “Ball Drop Viscosity Experiment Proposal,” 22-Feb-2019.
[139] W. R. Grimes, “REACTOR CHEMISTRY DIVISION ANNUAL PROGRESS REPORT FOR PERIOD ENDING DECEMBER 31, 1965,” United States, Mar. 1966.
[140] J. McDonald and H. T. Davis, “Determination of the Thermal Conductivities of Several Molten Alkali Halides by Means of a Sheathed Hot-Wire Technique,” *Phys. Chem. Liq.*, vol. 2, no. 3, pp. 119–134, Jan. 1971, doi: 10.1080/00319107108083807.
[141] S. Kitade, Y. Kobayashi, Y. Nagasaka, and A. Nagashima, “Measurement of the thermal conductivity of molten KNO3 and NaNO3 by the transient hot-wire method with ceramic-coated probes,” *High Temp. - High Press.*, vol. 21, no. 2, pp. 219–224.
[142] T. Omotani, Y. Nagasaka, and A. Nagashima, “Measurement of the thermal conductivity of KNO3-NaNO3 mixtures using a transient hot-wire method with a liquid metal in a capillary probe,” *Int. J. Thermophys.*, vol. 3, no. 1, pp. 17–26, Mar. 1982, doi: 10.1007/BF00503955.
[143] R. Tufeu, J. P. Petitet, L. Denielou, and B. Le Neindre, “Experimental determination of the thermal conductivity of molten pure salts and salt mixtures,” *Int. J. Thermophys.*, vol. 6, no. 4, pp. 315–330, Jul. 1985, doi: 10.1007/BF00500266.
[144] P. Jeschke, “Thermal Conductivity of Refractories: Working with the Hot-Wire Method,” ASTM International, West Conshohocken, PA, STP660-EB, Jan. 1978.

[145] J. E. Daw, J. L. Rempe, and D. L. Knudson, “Hot Wire Needle Probe for In-Reactor Thermal Conductivity Measurement,” *IEEE Sens. J.*, vol. 12, no. 8, pp. 2554–2560, Aug. 2012, doi: 10.1109/JSEN.2012.2195307.
[146] T. Omotani and A. Nagashima, “Thermal conductivity of molten salts, HTS and the lithium nitrate-sodium nitrate system, using a modified transient hot-wire method,” *J. Chem. Eng. Data*, vol. 29, no. 1, pp. 1–3, Jan. 1984, doi: 10.1021/je00035a001.
[147] M. Harada, A. Shioi, T. Miura, and S. Okumi, “Thermal conductivities of molten alkali metal halides,” *Ind. Eng. Chem. Res.*, vol. 31, no. 10, pp. 2400–2407, Oct. 1992, doi: 10.1021/ie00010a021.
[148] V. Ignatiev, A. Merzlyakov, V. Afonichkin, V. Khokhlov, and A. Salyulev, *Transport properties of molten-salt reactor fuel mixtures: the case of Na, Li, Be/F and Li, Be, Th/F salts*. Nuclear Energy Agency of the OECD (NEA): Organisation for Economic Co-Operation and Development - Nuclear Energy Agency, 2003.
[149] A. Redkin, Y. Zaikov, O. Tkacheva, and S. Kumkov, “Molar thermal conductivity of molten salts,” *Ionics*, vol. 22, no. 1, Nov. 2015, doi: 10.1007/s11581-015-1592-y.
[150] Q.-G. Zhao, S.-J. Liu, H. Guo, and X. Chen, *A theoretical model for predicting the thermal conductivity of binary molten salts*, vol. 92. 2016.
[151] F. F. Blankenship, “Reactor Chemistry Division annual progress report for period ending December 31, 1967,” *Oak Ridge Natl. Lab.*, p. 203, Mar. 1968.
[152] G. Mamantov, *Molten Salts: Characterization and Analysis*. Marcel Dekker, 1969.